THE UNIVERSITY
of EDINBURGH

Investigating the role of S-nitrosylation in plant antiviral defense

Muriel Monteiro

Doctor of Philosophy

The University of Edinburgh

2021

Table of Content

Declaration

The work presented in this thesis is the original work of the author. This thesis has been composed by the author and has not been submitted in whole or in part for any other degree.

Muriel Monteiro

Acknowledgements

I am extremely grateful to have had the opportunity to do my Ph.D. under the guidance of my supervisor, Dr. Attila Molnar. I am grateful that he took a chance on me, supported me, and guided me to help be the researcher I am today. I would like to thank my thesis committee, Dr. Elizabeth Bayne, and Prof. Andrew Hudson for their input and encouragement. I would like to extend my thanks to Prof. Steven Spoel for taking time out to discuss my project and giving valuable input.

I have had the pleasure of sharing lab space with wonderful people – Dr. Douglas Pyott, Dr. Fei Yue, Aron Ferenczi, Adéla Přibylová, and Yen Peng Chew. They have provided the much-needed moral support during my Ph.D., in addition to academic support. I am grateful for their patience, great conversations, and insightful suggestions. I would also like to extend my gratitude to all members of IMPS for their help and support throughout my time here.

I gratefully acknowledge The Darwin Trust of Edinburgh and the University of Edinburgh for funding my Ph.D. and giving me the opportunity to carry out research in Edinburgh.

My time in Edinburgh has taught me a great deal about science and life in general. I am very grateful to have had met loving, supportive people here - Alexander, Tine, Michelle, Thomas, Smitha, PK, and John. I am thankful for their companionship, support, and wisdom. I would like to especially thank Miqdad for his

support. Lastly but most importantly, I want to thank my family for their relentless support, encouragement, and unwavering faith in me.

Abstract

S-Nitrosylation, a post-translational modification, involves specific reversible incorporation of nitric oxide (NO) moiety to protein cysteine thiol to form an S-nitrosothiol (SNO). The cellular level of S-nitrosylation is maintained by S-nitroso glutathione reductase (GSNOR), an enzyme involved in the turnover of NO reservoir, S-nitroso glutathione (GSNO). Loss of function of AtGSNOR1 leads to increased SNO level and compromised immune response against bacterial and fungal pathogens. Similar consequences are observed in plants with excessive NO production. However, not much is known about the role of S-nitrosylation in antiviral response in plants which we aim to do in this study.

Arabidopsis mutants with varying level of nitric oxide (NO) and SNO: *gsnor1-3, gsnor1-3R, nox1, TRXh5 (nox1)* were selected. These mutants along with controls (Col-0, *eIF(iso)4E-1*) were inoculated with a Green Fluorescent Protein (GFP)-tagged potyvirus, Turnip mosaic virus (TuMV-GFP) to study susceptibility to viral infection. The susceptibility assay demonstrated higher viral resistance in plants with increased SNO levels. This observation contrasts with the observation made with bacterial and fungal pathogens.

Multiple facets associated with both host and pathogen were explored, to understand the underlying mechanism behind TuMV resistance in plants with higher SNO level. To achieve this, we focused on *gsnor1-3* mutants due to clearly displayed delayed viral infection, infection progression pattern and ease of viral inoculation.

This SNO mutant displayed slower onset of viral infection in rub-inoculated leaves, however viral replication rate and cell to cell movement was not hampered. We found that the systemic movement of TuMV was slower and delayed in gsnor1-3 plants. This was confirmed by evaluation of gsnor1-3 morphology that showed variation in plasmodesmata number, vascular pattern, and phloem transport rate, suggesting cumulative effect of host factors on delayed viral movement.

Abbreviations

a.u.	Arbitrary unit
ABA	Abscisic acid
AGO	Argonaut
APX	Ascorbate Peroxidase
APX1	Ascorbate peroxidase 1
ASC	Ascorbate
BR	Brassinosteroid
BS	Bundle sheath
CAT	Catalase
CC	Companion cells
CCA1	Circadian Clock Associated 1
CDPK	Calcium dependent protein kinase
CI	Cytoplasmic inclusion
CMV	Cucumber Mosaic Virus
COPI	Coat protein complex I
CP	Coat protein
CuLCrV	Cucurbit leaf crumple virus
DCL	Dicer-like
dpi	days pots inoculation
eIF	eukaryotic translation initiation factor

ERES	Endoplasmic reticulum exit sites
ETI	Effector-triggered immunity
GFP	Green fluorescent protein
GPX	Glutathione Peroxidase
GSH	Reduced glutathione
GSNO	S-nitrosylated glutathione
GSNOR	S-nitrosoglutathione reductase
GSSG	Oxidized glutathione
HC-Pro	Helper component proteinase
HR	Hypersensitive response
LHY	Late Elongated Hypocotyl
MAPK	Mitogen-activated protein kinase
MP17	Movement protein of potato leafroll virus
mRFP	Monomeric red fluorescent protein
NADPH	Nicotinamide adenine dinucleotide phosphate
NIa	Nuclear Inclusion a
NIb	Nuclear Inclusion b
NO	Nitric oxide
NOS	Nitric oxide synthase
nox1	NO overproducer 1
NPR1	Non-expressor of pathogenesis- related 1
NR	Nitrate reductase

ORF	Open reading frame
PAMPs	Pathogen associated molecular patterns
PCD	Programmed cell death
PCR	Polymerase chain reaction
PD	Plasmodesmata
PDLP1	Plasmodesmata localized protein 1
PPU	Plasmodesmata pore unit
PR proteins	Pathogenesis-related proteins
PRX	Peroxidase
PrxII E	Peroxiredoxin II E
PTI	PAMP-triggered immunity
PTM	Post translational modification
PVIP	Potyvirus VPg-interacting protein
RAV	Related to Abscisic Acid Insensitive 3 (ABI3)/Viviparous 1(VP1)
RBOH	Respiratory burst oxidase homolog
RNS	Reactive nitrogen species
ROS	Reactive oxygen species
RTM	Restricted Tobacco etch virus (TEV) movement
RT-qPCR	Reverse transcription-quantitative PCR
SA	Salicylic acid
SABP3	SA binding protein 3
SAR	Systemically acquired immunity

SE	Sieve elements
SEL	Size exclusion limit
SGS3	Suppressor of Gene Silencing 3
SNO	Nitrosothiol
SOD	Superoxide dismutase
sRNA	small RNA
TBRV	Tomato Black Ring Virus
TCV	Turnip Crinkle Virus
TEV	Tobacco Etch Virus
TGA1	TGACG motif binding factor1
TMV	Tobacco Mosaic Virus
TRSV	Tobacco Ringspot Virus
TRX h5	Thioredoxin h5
TuMV	Turnip Mosaic Virus
TVCV	Turnip Vein-Clearing Virus
VPg	Viral protein linked to genome
VRC	Viral replication center
vRNA	viral RNA
VSR	Viral suppressors of RNA silencing

Chapter 1: General Introduction

Plants have developed a suite of defence mechanisms to protect themselves from invading pathogens (Figure 1.1). Physical barriers such as cuticle, cell wall, in addition to chemical barriers such as secondary metabolites form the first line of defence (Lee *et al.*, 2017). Pathogens that successfully overcome these initial pre-formed barriers, can initiate a more complex two-layer immune response. The first layer of inducible defence in plants is triggered by either conserved pathogen-associated molecular patterns (PAMPs) or by host damage-associated molecular patterns (DAMP) (Newman *et al.*, 2013; Hou *et al.*, 2019). These molecules are recognised by pathogen recognition receptors (PRRs) present on the host cell surface to give rise to PAMP-triggered immunity (PTI) or DAMP-triggered immunity (DTI) respectively. However, well-adapted pathogens can interfere with PTI and promote infection by production of secretable molecules referred to as effectors. This in turn activates the second layer of inducible defence in plants, mediated by intracellular immune receptors (also known as disease resistance (R) proteins) that specifically recognise effectors, known as effector-triggered immunity (ETI) (Dangl and Jones, 2001; Kanyuka and Rudd, 2019).

Both PTI and ETI initiate a cascade of events such rapid burst of Ca^{2+} and reactive oxygen species (ROS), activation of Ca^{2+}-dependent protein kinases (CDPKs) and mitogen-activated protein kinases (MAPKs), extensive transcriptional and metabolic reprogramming (Yu *et al.*, 2017), to contain and terminate infection.

Additionally, ETI is associated with programmed cell death at site of infection, known as the hypersensitive response (HR) which limits pathogen spread (Mur *et al.*, 2008). ETI also induces the production and subsequent transport of mobile signals to uninfected systemic tissue, thereby imparting immunity to the whole plant. This phenomenon is known as systemic acquired immunity (SAR). It is characterised by increased accumulation of salicylic acid (SA) and production of anti-microbial pathogenesis-related (PR) proteins (Fu and Dong, 2013).

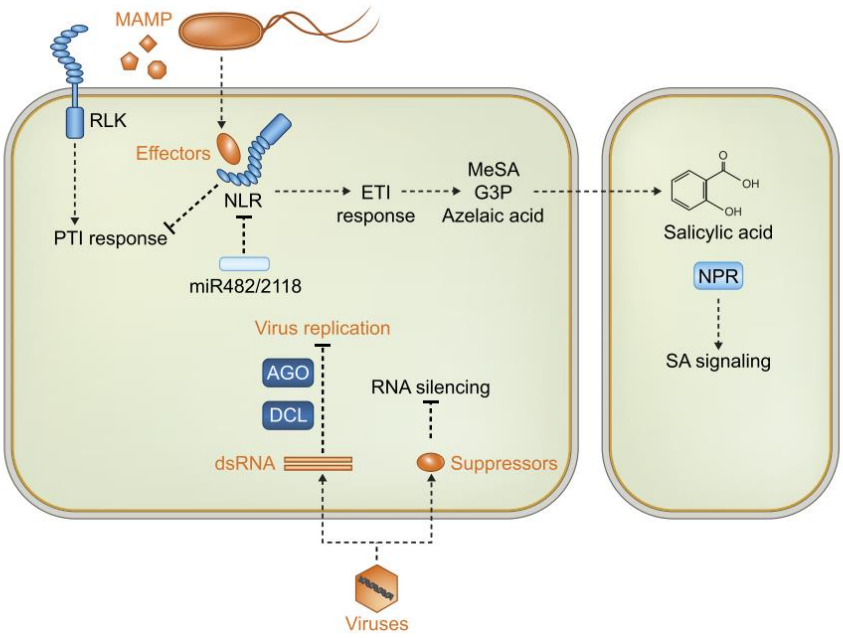

Figure 1.1 An overview of plant immune response (Han, 2019). The above figure depicts the inducible plant immune response against pathogens which involves PTI, ETI, SAR and RNA silencing.

In addition to protein associated triggers, plants have also developed immune response against invading nucleic acids known as RNA silencing. It involves silencing

of gene expression in a sequence specific manner by 21-25 nucleotide small RNA molecules (Baulcombe, 2004). RNA silencing is triggered by presence of double stranded RNA (dsRNA) in the cell, which could be a product of viral replication or a secondary-structure feature of single-stranded viral RNA (Baulcombe, 2004). These dsRNA are recognized and processed by Dicer-like (DCL) enzymes (Bernstein *et al.*, 2001) into 21-24 nucleotide small RNAs (sRNA) which guide Argonaut (AGO) proteins to silence the viral genome (Baumberger and Baulcombe, 2005; Carbonell *et al.*, 2012). Additionally, sRNAs are mobile and can prime non autonomous cells against viral infection (Voinnet and Baulcombe, 1997; Voinnet *et al.*, 1998).

Plant immunity is a complex process involving multiple players such as hormones, reactive oxygen and nitrogen species, post translational modification and RNAs (Pieterse *et al.*, 2009, 2012; Hua, 2013; Karapetyan and Dong, 2018). Many of these players are interdependent and can interact to fine tune an appropriate response against invading pathogens. This chapter focuses on role of redox particularly NO based S-nitrosylation, in plant immunity.

1.1 Role of Redox in plant immunity

Perception of pathogen leads to transient production of reactive oxygen and nitrogen species (ROS and RNS). Though cytotoxic at high concentration, at optimum concentrations, these reactive species play a key role in plant signaling. This section describes the importance of these redox molecules in plant immunity with emphasis on RNS.

1.1.1 Reactive oxygen species

Reactive oxygen species, formed by partial reduction of oxygen, include hydrogen peroxide (H_2O_2), superoxide (O_2^-) and hydroxyl radical (HO^-)(Grant and Loake, 2000). They are produced under both normal and stressed conditions in various subcellular compartments such as plasma membrane, cell wall, mitochondria, chloroplasts, and peroxisomes. Apoplastic ROS is mainly produced by plasma membrane localized NADPH oxidases known as respiratory burst oxidase homologs (RBOHs), cell wall peroxidases and amine oxidases. Whereas, intracellular ROS is produced in chloroplasts, and peroxisomes and to a less level in mitochondria (Das and Roychoudhury, 2014; Qi *et al.*, 2017).

Cellular ROS is maintained below toxic levels by a delicate balance between production and scavenging. The major ROS scavenging enzymes involved in ROS detoxification include superoxide dismutase (SOD), catalase (CAT), peroxidase (PRX), ascorbate peroxidase (APX), and glutathione peroxidase (GPX) (Torres *et al.*, 2006). In addition to these enzymes, ascorbic acid and glutathione play a major role in detoxification of O_2^- and H_2O_2 in a non-enzymatic manner (Mittler *et al.*, 2004).

Pathogen recognition results in biphasic ROS production with a weak transient first phase (ROS burst) followed by a stronger sustained second phase (Lamb and Dixon, 1997; Grant and Loake, 2000). The first, non-specific phase of ROS generation is produced in apoplast within minutes of pathogen (either virulent or avirulent) recognition. While, the second phase occurs few hours later, peaking at 6 hours after onset of infection (Zeng *et al.*, 2015). Phase II ROS production is specific

to avirulent pathogens and occurs in chloroplast (Liu *et al.*, 2007; Shapiguzov *et al.*, 2012).

On pathogen attack, ROS induces physiological changes such lignin cross linking, callose deposition and stomatal closure making cells physically resilient for pathogen entry (Lamb and Dixon, 1997; Qi *et al.*, 2017). As a signaling molecule, ROS can either directly modify sulfur-containing amino acid residues, such as cysteine and methionine, or indirectly modify targets through redox molecules (Qi *et al.*, 2017). Downstream signaling events associated with ROS sensing involve Ca^{2+} and Ca^{2+} binding protein, the activation of G-protein and the activation of phospholipid signaling. These events lead to differential gene expression by regulation of transcription factors including members of the WRKY, RAV and Myb families (Mittler *et al.*, 2004; Tripathy and Oelmüller, 2012). ROS signaling eventually results in genetic programs such as HR. This is evident in *Arabidopsis* mutants with downregulated *RBOH* where reduced ROS production leads to a lower HR against avirulent bacteria (Torres *et al.*, 2002).

The plant circadian clock is shown to be involved in the regulation of a variety of plant functions (Webb, 2003) and ROS homeostasis is no exception. Production of ROS, the activity of its scavengers, and transcription of ROS-responsive genes were shown to synchronously peak at specific times of the day. Further, loss of Circadian Clock Associated1 (CCA1) and Late Elongated Hypocotyl (LHY), core components of the plant circadian clock, impaired this rhythm (Lai *et al.*, 2012). This clearly demonstrates the involvement of the clock in ROS regulation. Similarly, the clock

regulates other plant immune components such as plant hormones and R genes (Covington *et al.*, 2008; Bhardwaj *et al.*, 2011; Wang *et al.*, 2011). Circadian regulation can therefore prime the plant for defence during specific times of the day, rendering the plants more susceptible to pathogens at other times of the day.

1.1.2 Reactive nitrogen species

1.1.2.1 NO synthesis

Multiple sources of NO have been identified, all of which fall into two main categories – oxidative or reductive pathways. Reduction of nitrite is considered to be a major source of NO production in plants. It can occur either non enzymatically – low pH, highly reducing conditions, or enzymatically - nitrate reductase (NR). Cytosolic NR is a rate limiting enzyme in nitrate assimilation, where it catalyzes reduction of nitrate to nitrite. It can further reduce nitrite to NO at a low rate under normal conditions. Under anoxic or acidic conditions, NO production by NR increases substantially (Rockel *et al.*, 2002). The model plant Arabidopsis has two NR isoforms coded by genes, *NIA1* and *NIA2*. Single and double NR mutant with low level of endogenous NO are compromised in NO associated functions such as stomatal movement, hormone responses, floral and root development (Desikan *et al.*, 2002; Kolbert and Erdei, 2008; Seligman *et al.*, 2008). Other sources of NO production via reductive pathway include plasma membrane bound NR, molybdoenzymes such as xanthine oxidases, aldehyde oxidases, and mitochondrial electron transport chain (Astier *et al.*, 2018).

Oxidative route of NO production involves conversion of arginine to citrulline. This reaction is catalyzed by nitric oxide synthase (NOS) in mammals. Though this route of NO production is also observed in plants, a NOS homologue has not been identified. Attempts to identify NOS homologue in plants lead to the identification of *NO associated 1 (noa1)* mutant with no NOS activity. It was later discovered that the gene responsible for impaired NO content in *noa1* was not NOS but a chloroplast targeted GTPase (Moreau *et al.*, 2008). Another *Arabidopsis* mutant, *NO overproducer 1 (nox1)* which has high levels of NO, displays high level of arginine and citrulline, supporting the notion of arginine dependent NO production (He *et al.*, 2004). Further, polyamines, which have arginine as precursor, have also been shown to trigger NO production (Tun *et al.*, 2006).

1.1.2.2 NO in plant immunity

NO has shown to be involved in multiple defense-associated functions either directly or via post translational modifications. NO functions as an antioxidant by reacting with highly cytotoxic, long lived O_2^- to give relatively less toxic, short-lived peroxynitrite ($ONOO^-$). Though peroxynitrite is a powerful oxidant, its deleterious effects are lesser than that of peroxides, making NO protective against ROS (Wink *et al.*, 1993). Furthermore, increased NO is shown to be associated with higher activity of antioxidant enzymes resulting in reduced H_2O_2 (Shi *et al.*, 2014). Thus, mitigating the negative effect of ROS. Conversely, NO acts alongside ROS to modulate defense responses. For example, HR is triggered only on balanced production of NO and ROS

(Delledonne *et al.*, 2001). Additionally, inhibition of NO synthesis during pathogen attack, reduced HR associated cell death (Delledonne *et al.*, 1998). NO is also reported to be involved in Ca^{2+} signaling, ABA-mediated stomal closure, MAPK activation and cGMP pathway (Domingos *et al.*, 2015; Ferreira and Cataneo, 2010).

A key route of NO bioactivity occurs through post translational modification (PTM) such as S-nitrosylation and tyrosine (Tyr) nitration. Tyrosine nitration is an $ONOO^-$ mediated modifications involving addition of a nitro group (NO_2) to protein tyrosine residue (Kolbert *et al.*, 2017). Tyrosine nitration of defense-associated pathogenesis-related proteins, PR-1, PR-3 and PR-5, indicate the role of this PTM in plant immune response (Takahashi *et al.*, 2016). Additionally, several proteins were identified to undergo Tyr nitration during hypersensitivity response (Cecconi *et al.*, 2009). Another NO based PTM, S-nitrosylation, is discussed in the section below.

1.2 S-Nitrosylation

S-nitrosylation refers to addition of NO moiety to a reactive thiol of cysteine (Cys) residues, forming nitrosothiol (SNO). S-nitrosylation is a specific reaction governed by multiple factors such local pH, redox status, presence of metal ions, flanking amino acid residues; that influence cysteine reactivity (Wang *et al.*, 2006). Hence, Cys residues in hydrophobic microenvironments or that are juxtaposed to acidic and basic residues are likely targets (Huber and Hardin, 2004). Screening known s-nitrosylated proteins in *Arabidopsis* has led to the identification of 3 possible motifs for S-nitrosylation : A-X(9)-C, C-X(6)-G, and C-X(2)-I (A= alanine, C= cysteine, G

=glycine, x = any amino acid) (Fares *et al.*, 2011). Such studies have helped develop computational tools to predict S-nitrosylation sites. Cross verification of computationally identified sites with those identified experimentally showed discrepancy between the two approaches (Chaki *et al.*, 2014). This is likely because the computational tools do not focus on protein structure, a dictating factor of Cys micro-environment and accessibility.

NO reacts with proteins with reactive cysteine to form S-nitrosylated proteins causing changes in protein structure and thus their function. Glutathione, a tripeptide antioxidant, is shown to easily react with NO to form S-nitrosylated glutathione (GSNO). In addition to releasing NO by homolytic cleavage (Singh *et al.*, 1996), GSNO can transfer their NO group to other protein thiols by a process known as transnitrosylation (Kovacs and Lindermayr, 2013). GSNO therefore allows NO to bring about signaling long after the stress induced NO is cleared up. Thus forming a more stable reservoir of NO bioactivity (Wang *et al.*, 2006).

1.2.1 Regulation of S-nitrosylation

S-nitrosylation is a reversible process. Removal of NO from s-nitrosothiol is known as denitrosylation which can occur enzymatically or non-enzymatically. Non enzymatic decomposition of s-nitrosothiols can be caused by light, reducing agents such as glutathione, pH, temperature and metal ions (Begara-Morales *et al.*, 2018). Enzymatic denitrosylation is carried out by reductases such as S-nitrosoglutathione reductase (GSNOR) and thioredoxins (TRX).

GSNOR has emerged as a major regulator of total cellular SNO levels. It catalyzes the denitrosylation of GSNO in a NADH-dependent reduction of GSNO to GSSG and NH_3 (Figure 1.2A). *Arabidopsis* mutant with loss of GSNOR1 function, *gsnor1-3*, shows increased accumulation of SNOs at basal level and upon pathogen infection, when compared to wild type (Feechan *et al.*, 2005). These mutants are compromised in multiple modes of immune response and were shown to be susceptible to bacterial and fungal pathogens. Overexpression of GSNOR1 in *gsnor1-3*, reversed pathogen susceptibility (Feechan *et al.*, 2005). Interestingly, GSNOR1 function itself is regulated by S-nitrosylation. This is likely to ensures NO signaling during stress-induced NO burst (Frungillo *et al.*, 2014; Guerra *et al.*, 2016).

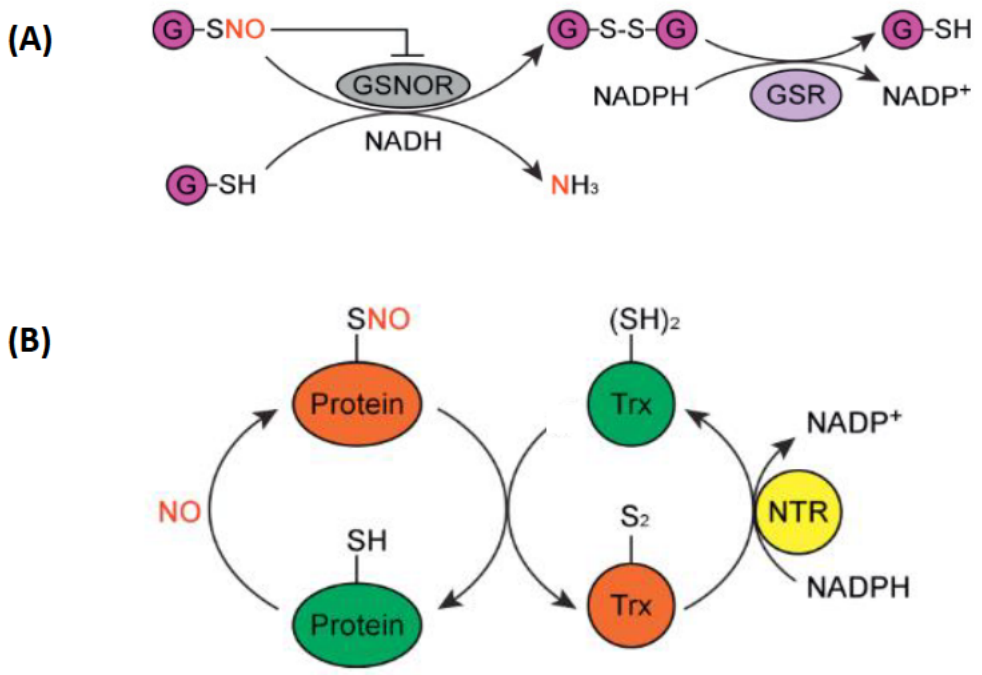

Figure1.2 Denitrosylation by GSNOR (A) and TRXh5 (B). (Feng *et al.*, 2019)

Thioredoxin superfamily that include conventional TRX, glutaredoxin (GRX), protein disulphide isomerase (PDI) and nucleoredoxin (NRX), catalyze reversal of diverse redox-based protein modifications. This is done through the conserved active site Cys-Gly-Pro-Cys, present in all members of the superfamily (Kortemme *et al.*, 1996). The first Cys of the active site attacks the oxidized thiol of the target protein leading to the formation of a mixed disulfide bond between TRX and its protein substrate. This mixed disulfide is reduced by the second Cys in the active site, resulting in the release of reduced protein substrate and oxidized TRX (Meyer *et al.*, 2008; Mata-Pérez and Spoel, 2019). Subsequent recycling of oxidized TRX occurs through cellular reductant such as NAPH-dependent TRX Reductase (NTR) and Ferredoxin-TRX Reductase (FTR) systems (Holmgren and Bjornstedt, 1995).

From the TRX superfamily, conventional TRX have emerged as important players in denitrosylation which can occur either via formation of mixed disulfide intermediates or by transnitrosylation (Benhar *et al.*, 2009). In *Arabidopsis,* thioredoxin h5 (TRX h5) has been reported to display denitrosylation activity via transnitrosylation mechanism (Figure 1.2B) (Kneeshaw et al., 2014). It uses only a single active cysteine from the TRX active site which is in contrast with the mammalian TRX which uses both the cysteines (Benhar *et al.*, 2008). Additionally, no mixed disulphide accumulation was detected during TRX h5 denitrosylation (Kneeshaw *et al.*, 2014). Overexpression of TRX h5 in *nox1* and *gsnor1-3,* rescued pathogen susceptibility in *nox1* but not in *gsnor1-3* mutant, indicating selective denitrosylation. TRX h5 and GSNOR1 are proposed to denitrosylate different set of S-

nitrosothiols based on the source of nitrosylation i.e. free NO or GSNO (Kneeshaw *et al.*, 2014).

1.2.2 Role of S-nitrosylation in plant immunity

Large scale proteomic approaches have facilitated the identification of around 1000 nitrosylated protein in *Arabidopsis*. These proteins cover a wide range of GO biological processes, including metabolism, abiotic and biotic stresses, cell organization, development, transport, energy process, signaling transduction, transcription and other processes (Lindermayr *et al.*, 2005; Romero-Puertas *et al.*, 2008; Fares *et al.*, 2011; Hu *et al.*, 2015). Though numerous proteins have been identified to be nitrosylated, relatively few of them have been functionally characterized.

Characterization of s-nitrosylated proteins have highlighted the role of S-nitrosylation in regulation of SA pathway, an important phytohormone in pathogen response (Figure 1.3). This is evident in *gsnor1-3* where SA induced gene expression is compromised leading to pathogen susceptibility (Feechan *et al.*, 2005). Non-expressor of pathogenesis- related 1 (NPR1), master regulator of SA-induced defense responses, is nitrosylated at Cys-156 which effects its localization. In an uninduced state, NPR1 exists as an oligomer connected by disulphide bond, in cytoplasm. On pathogen induction the disulphide bonds are reduced by TRXh5, to release NPR1 monomers that translocate to the nucleus to bring about SA-dependent gene expression (Mou *et al.*, 2003). S-nitrosylation of NPR1 stimulates oligomerization by

facilitating disulphide linkages between monomers, resulting in arrested gene expression (Tada *et al.*, 2008) (Figure 1.3). Further, activity of NPR1 interacting transcriptional factor, TGACG motif binding factor1 (TGA1), is also shown to be regulated by S-nitrosylation. TGA1 displays enhanced DNA binding activity in presence of GSNO (Lindermayr *et al.*, 2010). Additionally, S-nitrosylation of SA binding protein 3 (SABP3) inhibits its SA binding and carbonic anhydrase (CA) activity, the latter is required for the pathogen resistance (Wang *et al.*, 2009) (Figure 1.3).

S-nitrosylation was also shown to regulate PCD. S-nitrosylation of *At*RBOHD, decreases production of ROS, limiting cell death during hypersensitivity response (Yun *et al.*, 2011). S- nitrosylation of peroxiredoxin II E (PrxII E) inhibited both H_2O_2-reducing peroxidase activity and ONOO− detoxification, causing PCD on *Pseudomonas syringae pv. tomato* (Pst) infection by accumulation of toxic O_2− (Huang *et al.*, 2019). Activity of another antioxidant, ascorbate peroxidase 1 (APX1) is also shown to be governed by S-nitrosylation (Huang *et al.*, 2019).

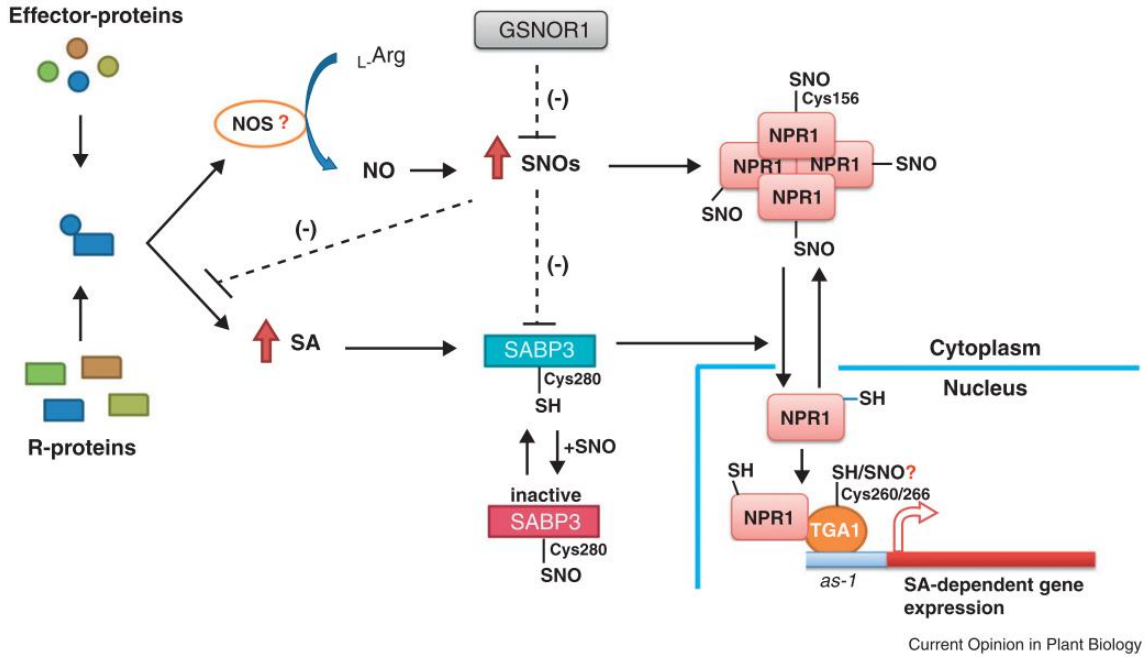

Figure 1.3 Regulation of SA signaling pathway by S-nitrosylation (Yu *et al.*, 2012). The schematic diagram shows different nodes of s-nitrosylation regulation of SA pathway – NPR1, master regulator of SA; TGA1, NPR1 interacting transcriptional factor; and SA interacting SABP3.

1.2.3 Role of S-nitrosylation in anti-viral response

In animals, multiple studies have indicated antiviral role of NO against DNA and RNA virus families, including Picornaviridae, Flaviviridae, Coronaviridae, Rhabdo-viridae, Reoviridae, Retroviridae, Parvoviridae, Herpesviridae, and Poxviridae (Colasanti *et al.*, 1999). NO is thought to bring about this function by S-nitrosylation of either viral or host proteins. For example, s-nitrosylation of coxsackievirus

protease 3C reduces both viral RNA and protein synthesis (Saura *et al.*, 1999). Additionally, virus encoded reverse transcriptase, ribonucleotide reductase, transcriptional factors, zinc finger domains, hemagglutinin, glycoproteins are shown to be targeted by NO to inhibit viral infection (Colasanti *et al.*, 1999). NO production by lymphocytes is reported to prevent re-activation of Epstein–Barr virus, possibly by regulation of redox-sensitive transcription factors, Zta and NF-KB (Mannick *et al.*, 1994).

In plants, the role of NO/S-nitrosylation in response against bacterial and fungal pathogens (above) is well researched. But when it comes to its role in plant viral responses, we have only just scratched the surface. Recent studies have implicated the role of NO in the plant viral response via the brassinosteroid (BR)-mediated pathway. In maize, BR pathway was shown to promote susceptibility to *Maize Chlorotic Mottle Virus* in a NO-dependent manner (Cao *et al.*, 2019). Whereas in *Arabidopsis,* NO was shown to bring about BR-mediated virus resistance against *Cucumber Mosaic Virus* (Li-Juan *et al.*, 2018). Contradiction in the two studies could be attributed to differences in host, viral family, or source of NO. In another study, application of NO-releasing compounds resulted in reduced symptoms and improved SAR in tobacco against *Tobacco Mosaic Virus* (TMV) (Song and Goodman, 2001). These studies highlight significant roles of NO in regulation of plant viral response. Yet no information on S-nitrosylation, a major form of NO based regulation, is available in this regard, which will be explored in this study.

1.3 Plant viruses

Plant viruses are obligate parasites that need living tissue for their multiplication. Simplistically, plant virions are made up of two primary components - the genome that is made of nucleic acid (DNA or RNA), and a protective covering that is made of protein (Gergerich and Dolja, 2006). On infections viruses can lead to various symptoms such as pattern of stripes or blotches; abnormalities in flower or fruit formation; leaf distortion, like leaf curling, and mottling; and other growth distortions, like stunting (Hamilton et al., 1981). These symptoms result in loss of yield and quality of crop and ornamental plants. Loss of yield due to plant viruses is estimated to cost more than $ 30 billion a year worldwide (Sastry and Zitter, 2014). This makes study of viruses, economically and agriculturally important. In this section, one such important genus of plant virus is discussed.

1.3.1 Potyvirus

Potyvirus is one of the largest plant virus genus comprising 30% of known species (Riechmann *et al.*, 1992). It belongs to second largest plant virus family *Potyviridae*, along with seven other genera. Potyviruses have a broad geographical distribution, a wide host range and can be transmitted by more than 200 species of aphids (Nigam et al., 2019). Potyviral infection of crop plants can lead to devastating yield loss. Thus, making it an economically and scientifically important virus group.

Potyviruses are non-enveloped, flexible filamentous particles (700 to 800 nm long). The virions are made up of helically arranged coat protein (CP) bound to

positive sense single stranded RNA. The viral RNA is covalently linked to viral protein linked to the genome (VPg) at the 5' end and is polyadenylated at the 3'end (Figure 1.4). It codes for a polyprotein precursor which undergoes cleavage to give 10 of 11 viral proteins (Riechmann *et al.*, 1992). The eleventh protein, P3N-PIPO is fusion protein synthesized separately from a short ORF embedded in P3 coding region (Chung *et al.*, 2008). Table 1.1 indicates the function of each of the viral proteins.

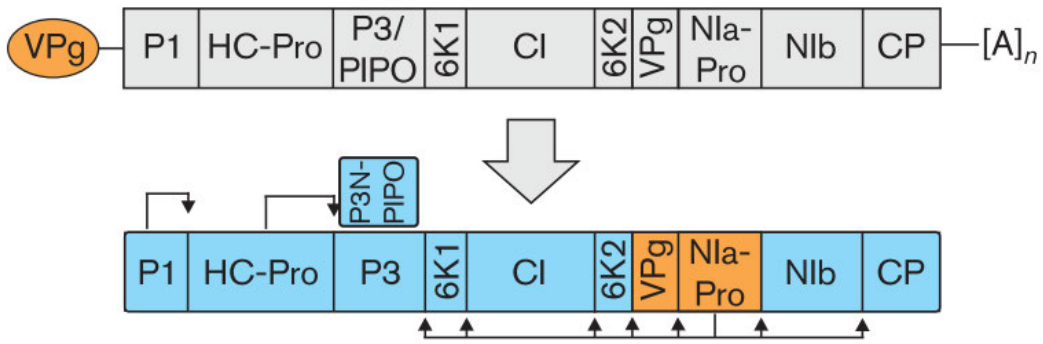

Figure 1.4 Schematic diagram of potyviral genomic RNA (grey) that translates to give polyprotein (blue). Proteolytic sites are marked with arrows indicating the names of the corresponding proteases (Ivanov *et al.*, 2014).

Table 1.1 List of potyviral proteins and their function (Revers and García, 2015; Nigam *et al.*, 2019).

Viral protein	Function
P1	Translation, modulator of replication
Helper component proteinase (HC-Pro)	Silencing suppression, aphid transmission and movement
P3	Virus replication and movement
P3N-PIPO	Cell-to-cell movement
6K1	Formation of replication vesicles
Cytoplasmic inclusion (CI)	Helicase involved in virus movement and replication
6K2	Formation of replication vesicles, Systemic movement
Viral protein linked to genome (VPg)	Translation, virus movement, and replication
Nuclear Inclusion a (NIa)	Polyprotein processing
Nuclear Inclusion b (NIb)	RNA-dependent RNA polymerase, Replication
Coat Protein (CP)	Virus movement, virion formation and aphid transmission

Turnip Mosaic Virus (TuMV) used in this study is a member of potyvirus genus. TuMV is transmitted in a nonpersistent manner by at least 89 aphid species (Walsh and Jenner, 2002). It has a broad host range and can infect up to 318 species in over 43 dicot families, including Cruciferae, Compositae, Chenopodiaceae, Leguminosae and Caryophyllace -ae. It is also known to infect monocots (Walsh and Jenner, 2002). Disease symptoms observed in infected plants vary based on the extent of infection. Early symptoms

include development of a mosaic pattern, shrinking, slight leaf stunting, mottling and chlorosis. At later stages of infection, severe stunting, chlorosis, necrosis, non-heading or loose heading and even withering of the entire plant is observed (Li et al., 2019). Such infections are known to cause up to 70% yield loss in crops.

1.3.2 Virus infection in plants

Viral infection in plants can be divided into 3 stages – viral translation and replication, cell-to-cell movement, and systemic spread. Upon entry into a host cell, virions are disassembled to release viral RNA (vRNA) which serves as template for both translation and replication. Interaction between 5' VPg of vRNA and eukaryotic translation initiation factor eIF4E or eIF(iso)4E is crucial in initiating viral infection using host translation machinery (Léonard *et al.*, 2000). *Arabidopsis* mutants lacking functional eIF(iso)4E, are resistant to potyviral infection (Lellis *et al.*, 2002).

Establishment of successful translation makes way for viral replication. Viral membrane spanning protein 6K2 initiates formation of viral replication centers (VRCs) at Endoplasmic Reticulum Exit Sites (ERES) using host coat protein complex I and II (COPI and COPII) machinery (Wei and Wang, 2008). As the infection proceeds, the VRCs use the host actomyosin system to move and fuse to chloroplast which is thought to be the site of active replication (Mäkinen and Hafrén, 2014). VRCs form a protective microenvironment for viral replication, containing factors required for replication i.e P3, CI, CI–6K2, 6K2–NIa, NIaPro and NIb (Revers and García, 2015). Additionally, several host proteins associated with viral translation, such as

eukaryotic initiation factor 4E (eIF4E), eukaryotic elongation factor 1A (eEF1A), RNA helicase-like protein RH8, poly(A) binding-protein (PABP), and heat shock protein 70 (HSP70), were also identified in VRCs (Mäkinen and Hafrén, 2014). Identification of both translation and replication factors in VRCs indicates that the two events are coupled.

To cause a successful infection, viruses must move from point of entry to the rest of the plant. Viral spread is initiated by movement of viruses to neighboring cells till they reach the vasculature. Once in the vascular tissue, viruses hijack the plants transport system (xylem and phloem) to reach systemic tissue.

Cell-to-cell movement of viruses occurs through plasmodesmata (PD), cytoplasmic channels that connect the neighboring plant cells (Figure 1.5). PD is permeable and allows molecules that fall within the size exclusion limit (SEL) to diffuse (passively) through it. PD permeability can be increased by dilation or active gating or structural remodeling to allow the passage of larger molecules (Roberts and Oparka, 2003; Sager and Lee, 2018). This mechanism is exploited by viruses for their spread. Potyviral CI is targeted to PD in P3N-PIPO dependent manner using functional host secretory pathway. At PD, CI forms conical structures that are anchored to PD by P3N-PIPO, allowing movement of viral particles (Wei *et al.*, 2010). Potyviral proteins CP (Dolja *et al*., 1994) and HC-Pro (Klein *et al*., 1994) are also shown to be necessary for cell-to-cell movement by deletion/mutation studies.

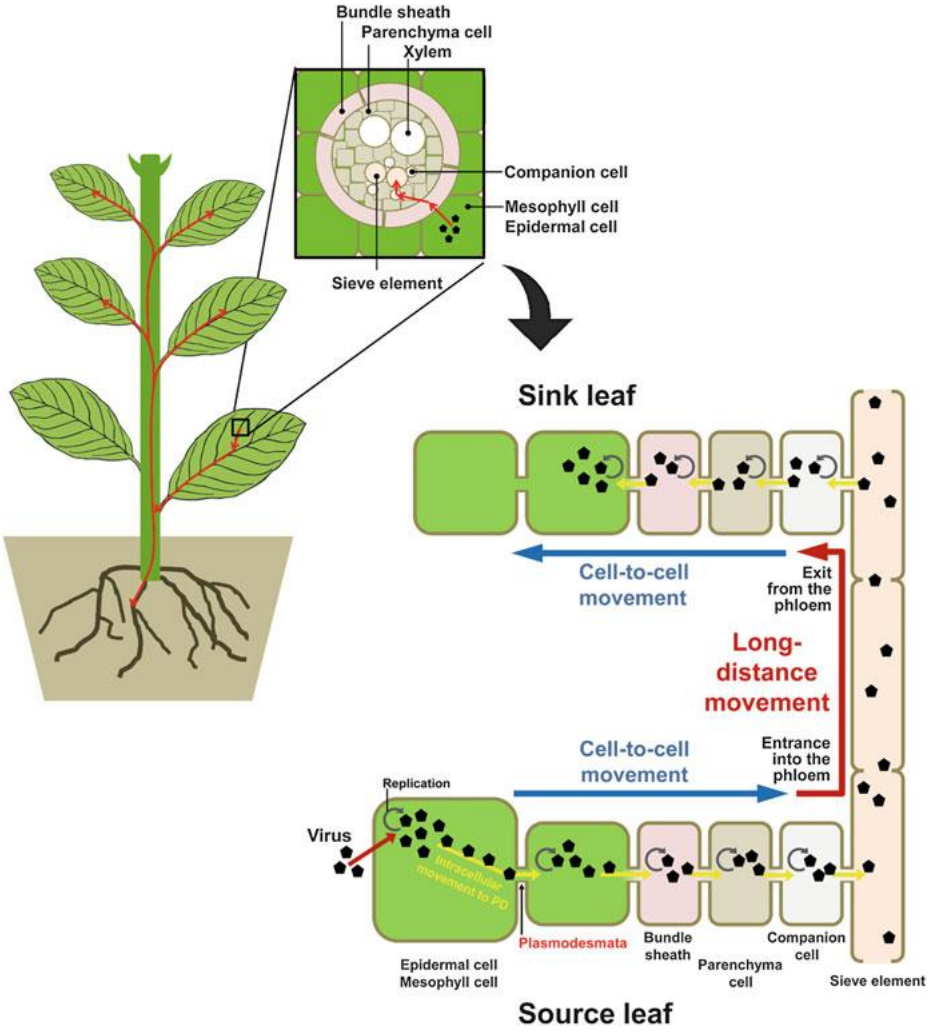

Figure 1.5 Viral infection in plants (Wang and Zhou, 2016). On entry within a cell, virus replicates itself. It then moves to neighboring cells via PD till it reaches the phloem for systemic transport.

Systemic movement of potyviruses in plants mostly occurs through phloem and follows the source to sink transportation pattern of carbohydrates (Figure 1.5). Recent evidence shows that potyviruses can also make use of xylem for long distance movement (Wan *et al.*, 2015). The exact molecular mechanism of viral systemic

movement is not well understood. However, viral and host factors involved in the process have been identified. Potyviral CP, VPg, 6K2 and HC-Pro are shown to play crucial role in systemic movement (Urcuqui-Inchima *et al.*, 2001; Hipper *et al.*, 2013). In *Arabidopsis, SHA*3 and *RTM* genes are involved in potyvirus long-distance transport (Hipper *et al.*, 2013; Revers and García, 2015).

Chapter 2: Materials and methods

2.1 Plant material and growth conditions

Arabidopsis thaliana seeds were stratified in 1.5ml Eppendorf tubes containing water, in dark at 4℃ for 2-3 days. Stratified seeds were sown on Levington F2+S professional growth compost. The plants were grown in controlled growth chambers at 21℃ with 16h/8h light/dark cycle.

Nicotiana benthamiana seeds were directly sown on the growth compost and grown in the conditions mentioned above.

Table 2.1 *Arabidopsis* mutant lines used.

Mutant line	Gene locus	Source	Reference
gsnor1-3	At5g43940	Gary Loake	Feechan *et al*.,2005
35S: FLAG GSNOR1 (gsnor1-3R)	At5g43940	Gary Loake	Feechan *et al*.,2005
nox1	At5g33320	Gary Loake	He *et al.*, 2004
TRXh5 (*nox1*)	At5g33320	Steven Spoel	Kneeshaw *et al*.,2014
eIF(iso)4E	At5g35620	Christophe Robaglia	Duprat *et al*., 2002

2.2 Sap collection and rub inoculation

Agrobacterium cells carrying a plasmid TuMV-GFP (Turnip mosaic virus tagged with green fluorescent protein) dissolved in infiltration media (10mM MES pH5.6, 150µM acetosyringone, 10mM $MgCl_2$) were syringe infiltrated into 3-week-old *N. benthamiana* leaves at OD_{600}=0.5. TuMV - GFP infected sap was collected from systemic leaves of infected *N. benthamiana* plants 7-9 days post inoculation (dpi).

Leaves were harvested and ground with three volumes of 1mM sodium phosphate buffer (pH7.0) in chilled mortar. It was then transferred to a 15ml falcon tube and centrifuged at 3000rpm for 10 min to pellet plant debris. The supernatant was aliquoted into 1.5ml Eppendorf tubes, flash frozen in liquid N_2 and stored at -80°C till further use.

For *Cucumber mosaic virus* (CMV), RNA1, RNA2 and RNA3 were transcribed *in vitro* (2.4), mixed in equal concentration and rub inoculated on 3-week-old *N. benthamiana* leaves using aluminum oxide powder as abrasive. CMV infected sap was collected at 7 dpi as described above.

For *Arabidopsis* infections, abaxial leaf surface of 3- 4-week-old plants was dusted with aluminum oxide powder and 5µl of viral sap was applied by rub inoculation. Leaf five, six and seven counted from the top of the rosette were inoculated on each plant. All inoculations were carried out 8 hours after dawn for high infectivity.

2.3 Imaging of GFP fluorescence

GFP expression was monitored using a BlakRay handheld mercury UV lamp. The plants were photographed by Canon G16 camera at long exposure setting i.e shutter speed 6s and ISO 160.

2.4 In vitro transcription

CMV plasmids, pF109, pF209 and pF309 (ref) were linearized by Pst1 restriction enzyme. Since Pst1 produces 3' overhangs which are not ideal for in vitro transcription, digested plasmids were blunted by Klenow large fragment. The plasmids were then purified by phenol/chloroform method as follows. Equal volume of phenol: chloroform: isoamyl alcohol (25:24:1) was added to the digestion/blunting reaction mix, vortexed and centrifuged at 13,000rpm for 10 minutes. The aqueous phase was transferred to a fresh Eppendorf tube and mixed with equal volume of chloroform: isoamyl alcohol (24:1) and centrifuged at 13,000rpm for 5 minutes. This step was carried out twice. To the aqueous phase collected in a fresh Eppendorf tube, 2.5 volumes of ethanol and 1/10th volume of 3M sodium acetate pH 5.2 was added. The samples were mixed by inversion and incubated on ice for 30 minutes. Plasmid was pelleted by centrifugation at 13,000 rpm for 30 minutes. The pellet was washed with 80% ethanol. Any residual ethanol was pipetted outed after a quick centrifugation. The pellet was air dried and re-suspended in 25µl of RNase-free water.

In vitro reaction mix was prepared at room temperature by adding reagents in the following order - 1X T7 transcription buffer (Promega), 10 mM DTT, 50 units RNaseOUT Recombinant Ribonuclease Inhibitor (40 U/µL; Invitrogen), 2.5 mM rATP, 2.5 mM rUTP, 2.5 mM rCTP, 0.25 mM rGTP, 1mM m7G(5')ppp(5')G RNA Cap Structure Analog (NEB), 1µg linear DNA template, 100 units T7 RNA Polymerase (20 U/µL; Promega) and 30mM MgCl2 in a total volume of 50 µL. Reaction was incubated at 37℃ for 15 minutes. 2mM rGTP was added to the reaction, followed by incubation at 37℃ for 1hour 45 minutes. 3µl of transcription product was mixed with 2X RNA

loading dye (10 mM EDTA, 0.10% bromophenol blue and 0.10% xylene cyanol in 100% (v/v) deionized formamide), denatured at 65℃ for 5 min, then loaded on 1% agarose gel to be analyzed.

2.5 Plant DNA/RNA purification

Total nucleic acids (TNA) were purified from plant tissue or protoplasts by phenol/chloroform extraction using a method adapted from White & Kaper, 1989. Plant tissue was collected in 2mL Eppendorf tubes containing two metal ball-bearings and frozen in liquid nitrogen. Plant tissue was ground in pre-chilled blocks in a Qaigen Tissue Lyzer (Qaigen). 600µL of Tris-buffered water-saturated phenol (pH 8.0) and 600µL of TNA extraction buffer (100mM Glycine, 100mM NaCl, 2% SDS, 10mM EDTA, pH 9.5) was added to the powdered plant tissue. The samples were vortexed and then centrifuged at 13, 000 rpm for 10 minutes. The aqueous phase was transferred to a fresh 1.5ml Eppendorf tube containing 600µL of phenol: chloroform: isoamyl alcohol (25:24:1), vortexed and centrifuged as before. This step was repeated twice. 500µL of aqueous phase was then transferred to a new tube containing 500µL of chloroform: isoamyl alcohol (24:1), vortexed and centrifuged at 13, 000 rpm for 5 minutes. 400µL of aqueous solution was transferred to a tube and TNA was precipitated in 1 mL absolute ethanol and 40µL 3 M sodium acetate (pH 5.2). Samples were mixed by inversion followed by incubation on ice for 30 minutes. TNA was pelleted by centrifugation at 13, 000 rpm for 30 minutes at 4℃. The pellet was washed with 1 mL 80% ethanol. Any residual ethanol was pipetted outed after a quick

centrifugation. The pellet was air dried and re-suspended in 50µL of RNase-free water. The concentration of the TNA was determined using a Nanodrop. The RNA quality was checked by mixing 2.5µL of sample with 2X RNA loading dye, heating the samples at 65℃ for 5 minutes, and separating the TNA on a 1 % agarose gel.

2.6 DNase treatment and cDNA synthesis

3µg of TNA was treated with Turbo DNase (Invitrogen) to remove DNA according to the manufacturer's instruction. cDNA was synthesized from 1µg of RNA using random hexamer primers and SuperScript II reverse transcriptase (Life Technologies), according to manufacturer's instruction.

2.7 Quantitative RT-PCR (qRT-PCR)

Quantitative RT-PCR analysis was carried out with SYBR Green I Master Mix on LightCycler®480 thermocycler (Roche) using gene-specific primers (Table 2.2). 10µL reaction was set up containing 1X SYBR green master mix, 0.1µM forward primer, 0.1µM reverse primer and 0.3µL cDNA. Three technical replicates were performed for each gene per sample analyzed. The following cycling conditions were used for all reactions: 95℃ 5 min > (95℃ 10s > 60℃ 10s > 72℃ 15s) x 45. For cDNA prepared from protoplasts samples, 0.5µL cDNA was used per reaction. The data obtained for qRT-PCR was analyzed using LightCycler®480 software for relative quantification of gene of interest.

2.8 Oligonucleotides

Oligonucleotides were ordered from Integrated DNA Technologies, Inc. and re-suspended in sterile distilled water to obtain a 100µM stock solution. All oligonucleotides were designed such that the annealing temperature was 60℃.

Table 2.2 List of oligonucleotides used in this study.

Oligonucleotide name	Sequence (5'-3')	Used for
AtEF1a_FP	CACCACTGGAGGTTTTGAGG	qRT-PCR
AtEF1a_RP	TGGAGTATTTGGGGGTGGT	qRT-PCR
TuMV_CP_FP	GTGGCTCTAAACCTCGATCAT	qRT-PCR
TuMV_CP_RP	AACCATGTGTCAAACTGCTTTC	qRT-PCR
mcherry_FP	GACTACTTGAAGCTGTCCTTCC	qRT-PCR
mcherry_RP	CGCAGCTTCACCTTGTAGAT	qRT-PCR
CMV_RNA1_FP	CAGTGTTGTTCACGCACTATTC	qRT-PCR
CMV_RNA1_RP	CATTCCTCTCCACCGTCAAA	qRT-PCR
CMV_CP_FP	CCTTTGTAGGGAGTGAACG	qRT-PCR
CMV_CP_RP	CCCACACGGTAGAATCAA	qRT-PCR
GSNOR_FP	GGTCTCTTTCCTTGTATTCTAG	qRT-PCR
GSNOR_RP	GCATTCACGACACTCAGCTTG	qRT-PCR
TRXh5_FP	CATACCCTCGAAGTTTGGAACGAGA	qRT-PCR
TRXh5_RP	TTGCCTCAACTTTGAATTCCTGAGC	qRT-PCR
gsnor1-3_FP	CACAGCCTCAAATTGATTCAC	genotyping
gsnor1-3_RP	ATAATAACGCTGCGGACATCTAC	genotyping

2.9 Venation pattern analysis

Leaf four, seven and ten, counted from the top of a 4-week-old Arabidopsis rosette were cleared to analyze vasculature pattern in Col-0 and *gsnor1-3*. Leaves were incubated in 100% ethanol at 4℃, overnight, for clearing out chlorophyll pigment. If complete clearing was not achieved after overnight incubation, ethanol was replaced with fresh ethanol and the leaves were incubated further till complete clearing was achieved. Leaves were then rehydrated by a series of one-hour incubations at room temperature, first with 70% ethanol, followed by 50% ethanol. Cleared leaves were mounted onto a slide, covered by a cover slip and observed under Leica MZ 16 F stereomicroscope. Leaves were imaged using Canon G16 camera under darkfield illumination, 0.71 magnification. The images were then analyzed using PhenoVein software as described by Buhler *et.al.,* 2015.

2.10 Phloem assay

Soil grown, 12-day old *gsnor1-3* and 10-day old Col-0 seedlings were used for this assay. The seedlings were imaged to calculate surface area using Image J. The assay was carried out only if there was no significant difference between the seedling surface area of Col-0 and *gsnor1-3.*

Cotyledons were treated with 1µL of 2.5% (v/v) Adigor (Syngenta) solution for 1 hour, following 1µL of 9mg/mL Esculin for 4 hours. Cotyledons were washed in 700µL of absolute ethanol (Wash) and then collected in a separate tube containing 700µL of absolute ethanol (Cotyledon). The true leaves were collected in a third tube

containing 700µL of absolute ethanol. All tubes were heated to 75°C for 1 h, chilled on ice briefly, and then centrifuged at full speed for 2 min. Samples were split into 200µL portions and loaded into separate wells in a 96-well plate (Greiner) before being read on FLUOstar® Omega with excitation set at 355 nm and emission collected at 460 nm for Esculin. Control samples from seedlings not treated with Esculin were used to give background readings and subtracted from all samples. Five seedlings were pooled to form one sample.

2.11 Protoplast assay

Protoplast isolation was carried out using the tape-Arabidopsis sandwich method (Wu *et al.*, 2009). Adaxial surface of leaves from 3-4 week old Arabidopsis plants were gently placed onto strips of autoclave tape attached to sterile work bench. Stripes of magic tape was then stuck to the abaxial surface of the leaves and slowly removed to strip the lower epidermis and expose the mesophyll cells. The autoclave tape was incubated in a petri plate containing 12ml enzyme solution (20 mM MES pH 5.6, 10mM $CaCl_2$, 20mM KCl, and 400mM D-mannitol, 0.1% BSA, 0.3% Macerozyme R-10 and 0.5% Cellulase R-10 (Yakult)) with leaf side down, for 2 hours at 50 rpm, 25°C. The tape was removed and 5ml of W5 solution (150mM NaCl, 125mM $CaCl_2$, 5mM KCl, 5mM Glucose and 2mM MES pH 5.6) was added and mixed by gently swirling the petri plate. Protoplasts were then transferred to 50ml tubes and centrifuged at 100Xg for 3 minutes. Supernatant was carefully removed, and the protoplasts were re-suspended in 15ml W5 solution. Protoplasts were rested on ice

for 30 minutes, until transfection. Following protoplast yield assessment by hemocytometer, protoplast were centrifuged as before and re-suspended in MMg solution (4mM MES pH 5.6, 15mM $MgCl_2$ and 400mM D-mannitol) to a concentration of 10^6 cell/ml.

For PEG mediated transfection, 90µg of plasmid was mixed with 15 X 10^5 cells in a 15ml tube. Equal volume of PEG solution, pH 8-9 (40% PEG4000, 200mM D-mannitol and 100mM $CaCl_2$) was added, mixed gently by inversion and incubated at 25°C for 10 minutes. Two volumes of W5 solution was added, mixed by inversion and centrifuged at 100Xg for 3 minutes. Supernatant was carefully discarded, and the pellet was re-suspended in 3ml of storage solution (5% fetal bovine serum (Gibco), 50 µg/ml carbenicillin in W5 solution). Protoplasts were split into 3 portions i.e. 1ml with 5X10^5 cells and stored in 6 well plates at 25°C in dark till sample collection.

2.12 Crossing and genotyping

Unfertilized PDLP1 mRFP X MP17 GFP carpels were cross-pollinated with Col-0 or *gsnor1-3* pollen. Plants from cross pollinated siliques (F1 generation) were genotyped (Table 2.2) using Phire Plant Direct PCR Master Mix (Life Technologies), according to manufacturer's instruction.

2.14 Particle bombardment

50mg of gold particles (0.1µm) were suspended in 1ml sterile water and vortexed vigorously for 1-2 minutes. The suspension was centrifuged at 13,000rpm for 1 minute. The pelleted gold particles were washed three times with 100% ethanol and once with sterile water. Washed pellet was resuspended in 1ml sterile water, divided into aliquots of 25µl per 1.5ml eppendorf tube and stored at 4°C till further use.

5µg of plasmid and 62.5µl of 1M $CaCl_2$ was added to the tube containing 25µl gold suspension. Each addition was followed by brief vortex for mixing. Further, 10µl of 0.1M spermidine was added to the tube and mixed in by vortexing at 15-20 Hz for 2 minutes. The tube was then incubated on ice for 20 minutes, followed by centrifugation for 10s to pellet the DNA-coated gold particles. The pellet was washed with 180µl of 100% ethanol and finally resuspended in 100µl of 100% ethanol.

5µl of DNA-coated gold particle suspension was loaded onto the centre of the microcarrier for leaf bombardment using a custom built gene gun as described in Gaba and Gal-On (2005). Attached leaf of a 4-week-old Arabidopsis plant was bombarded by placing it 1-2cm away from the nozzle of the gene gun at a pressure of 2bar. A single loading was used to bombard 3 leaves of a single plant.

2.15 Confocal microscopy

Leaves to be analyzed were mounted on slides with double side tape and imaged using a Leica SP2 confocal laser scanning microscope with a ×40 water dipping

lens (Leica Microsystems). GFP was excited using a 405-nm laser and mRFP/mCherry was excited using a 488-nm laser. Confocal images were then analyzed using ImageJ to obtain plasmodesmata count and foci area.

Chapter 3: Plants with elevated SNO levels are more resistant to TuMV infection.

3.1 Introduction

S-nitrosothiol level in plants have shown to effect different defense pathways – Non host disease resistance (NHR), R gene mediated immunity and Basal immunity. Study carried out using bacteria, fungus and oomycete (*Blumeria graminis*, *P.syringae* pv. *Phaseolicola, P. syringae* DC3000 and *Hyaloperonospora parasitica*) in *Arabidopsis* mutant *gsnor1-3* identified requirement of GSNOR1 for optimum NHR and R gene-mediated immunity (Feechan et al. 2005). Functional GSNOR1 is required for the maintenance of cellular SNO homeostasis by reduction of NO bio-reservoir, GSNO. Dysfunctional GSNOR1, therefore leads to an increase in cellular SNO level. Similar disease phenotype was seen in loss-of-function mutant *nox1* which has high level of SNO due to over production of NO (Yun et al. 2016).

Pathogen susceptibility observed due high SNO content can be reversed by over expression of reductases involved in denitrosylation process. Over-expression of GSNOR1 in *gsnor1-3* plants (referred to as *gsnor1-3R* in this study) was able to rescue plant susceptibility to pathogens (Yun et al. 2016). Similarly, over-expression of another reductase enzyme, TRXh5 was able to rescue disease phenotype in *nox1* (Kneeshaw *et al.*, 2014). Taken together, S-nitrosylation influences plant immunity against bacterial and fungal pathogens at multiple levels. However, the role of S – nitrosylation in plant anti-viral responses has not yet been investigated.

In this chapter we identify a role of S-nitrosylation in plant anti-viral response by subjecting the *Arabidopsis* mutants described above to a viral susceptibility assay. We demonstrate an inverse correlation between SNO level and viral infection.

3.2 Results

3.2.1 Optimization of viral infection

Wild-type (WT) *Arabidopsis* plants, *Col-0*, were inoculated with *Turnip Mosaic Virus* tagged with green fluorescent protein (TuMV-GFP) to optimize viral infection. TuMV- GFP is a well-characterized recombinant virus that allows easy identification of infection pattern via GFP reporter under UV light (Garcia-Ruiz *et al.*, 2010).

A combination of different tools, abrasive agents and site of infection were used to determine the most efficient way to infect plants with virus. Two abrasives – carborundum (SiC) and aluminum oxide (Al_2O_3); and five tools/methods–Rub inoculation, cotton bud, toothbrush, sponge, and Velcro, were examined. Both adaxial and abaxial surfaces of the leaf were tested for infection rate.

24 plants (Col-0) were tested for each method of infection. Of the 24 plants, 12 plants were infected on the adaxial leaf surface and remaining 12 plants on the abaxial leaf surface. Powdered aluminum oxide proved to be more efficient than carborundum in causing mechanical damage required for viral infection (Figure 3.1A). Of the methods tested rub inoculation worked best on the adaxial side while the use of cotton bud and Velcro were most efficient on the abaxial side. Treatment on the adaxial side of the leaf demonstrated to work better for all tested methods (Figure 3.1B). Therefore, for future experiments, aluminum oxide dusted adaxial surface of the leaf was rub inoculating with infectious viral sap.

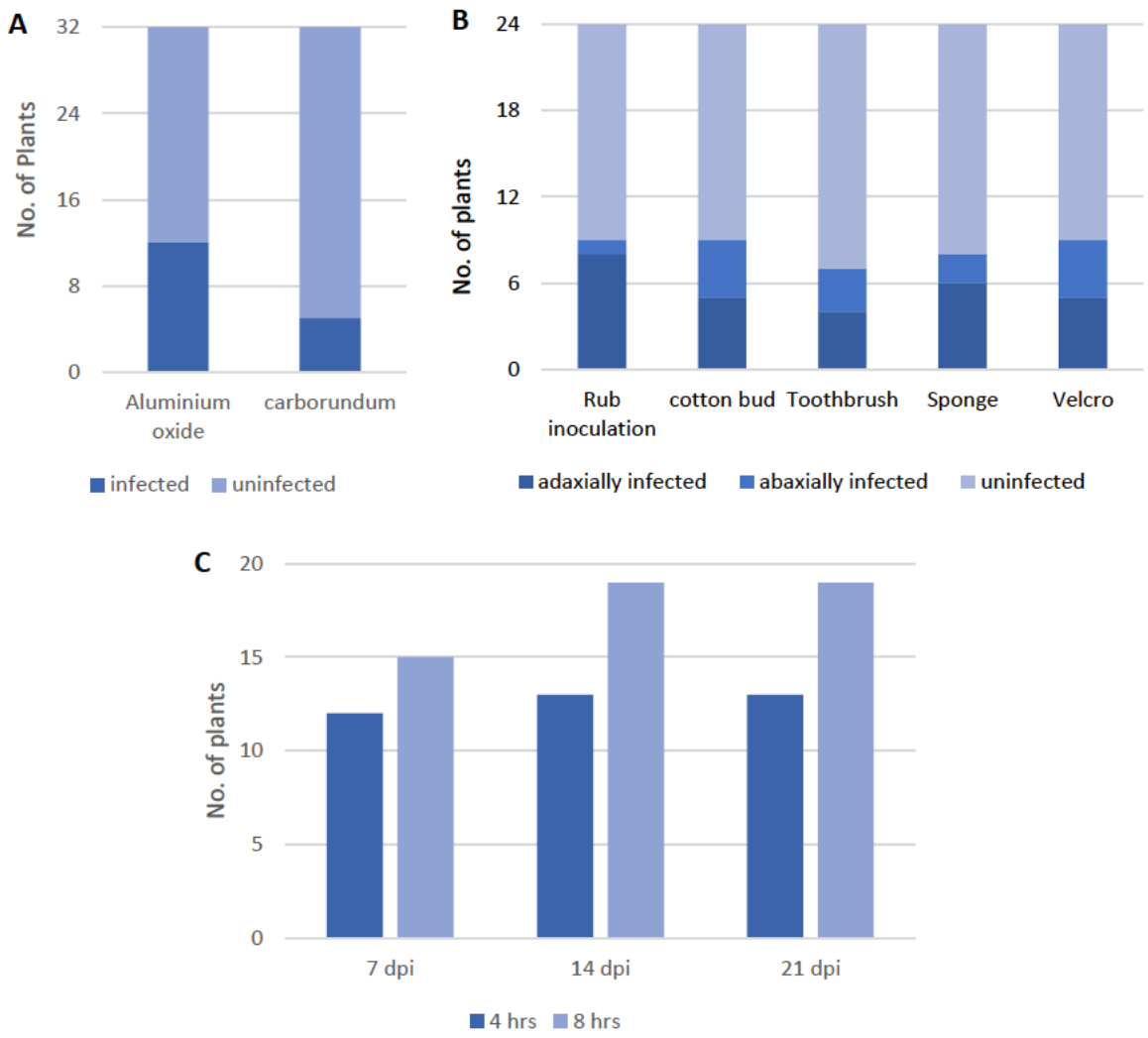

Figure 3.1 Optimization of viral infection. Col-0 plants were inoculated with TuMV-GFP to optimize mode of mechanical damage (A), method B) and time (C) of inoculation. (A) Aluminum oxide and carborundum were tested for their efficiency as an abrasive for viral inoculation. (B) Methods of viral inoculation (rub inoculation, cotton bud, toothbrush, sponge, and Velcro) and site of inoculation (adaxial or abaxial) were tested. (C) Time of viral inoculation leading to higher probability of viral infection was tested. For each of the test experiments 20-24 plants were used.

Circadian rhythm is known to influence plants ability to fend off pathogens (Hua, 2013). In our trial experiments, we noticed different rate of infection was achieved when plants were inoculated in the morning vs afternoon. Based on this observation, two inoculation time points were tested for infection efficiency - 4 and 8 hours after dawn. As shown in figure 3.1C, plants inoculated 8 hours after dawn showed higher rate of infection. Therefore, infectious sap was rub inoculated on adaxial surface of the aluminum oxide dusted leaf in subsequent experiments, 8 hours after dawn.

3.2.2 TuMV susceptibility assay

To investigate effect of S-nitrosylation on plant anti-viral response, *Arabidopsis* mutants with varying level of NO and SNO content (table 3.1) were infected with TuMV-GFP (Figure 3.2). Every test genotype was paired with a rescue genotype as seen in case of bacterial infections – *gsnor1-3* with *gsnor1-3R*; *nox1* with TRXh5(*nox1*). *Arabidopsis* mutant *eIF(iso)4E*, resistant to TuMV, was used as negative control. Mutants *nox1* and TRXh5(*nox1*) were sown a week prior to other genotypes due to slower development.

Inoculated plants were monitored for progression of infection for a duration of 3 weeks with periodic sample collection. Two approaches were then used to evaluate viral resistance in plants – percentage of plants infected in the population and quantification of viral RNA by qPCR (Figure 3.2). In order to get a true

representation of infection at population level via qPCR, 9-10 inoculated plants were randomly selected and pooled together to form one sample at each time point.

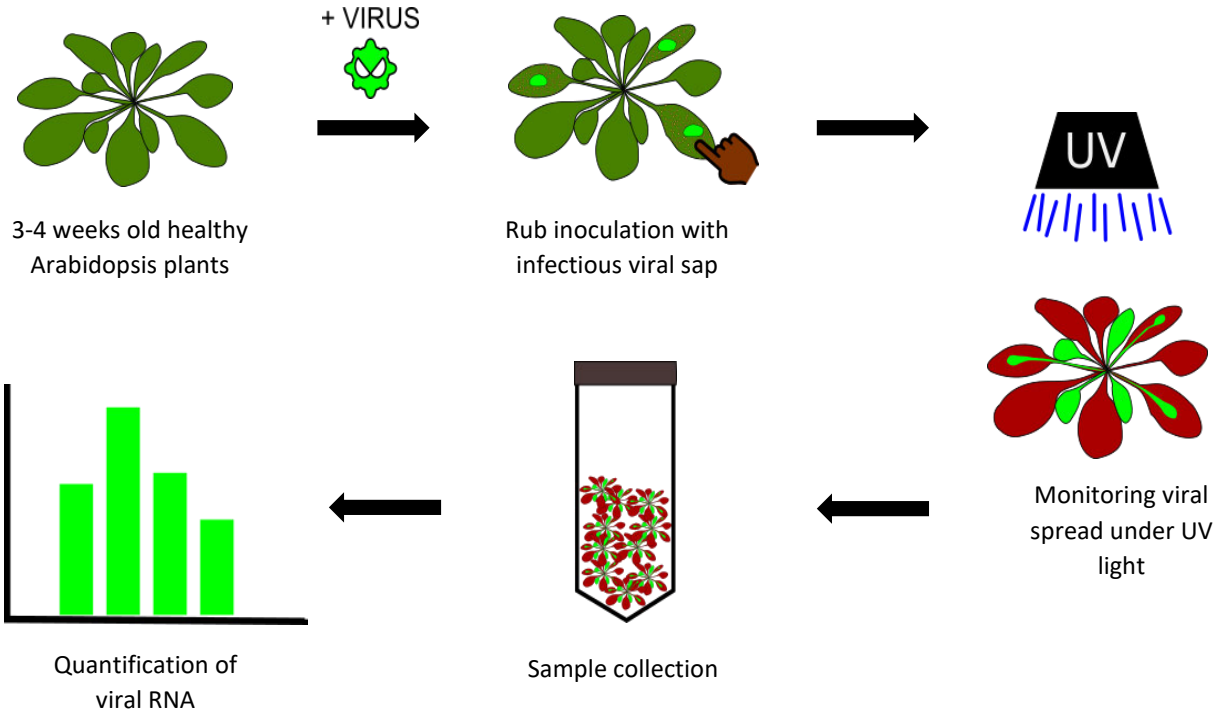

Figure 3.2 Schematic diagram of TuMV susceptibility assay. Healthy *Arabidopsis* plants were inoculated with TuMV-GFP. Spread of viral infection was monitored under UV light and samples were collected at periodic intervals to quantify viral load.

Table 3.1: List of S- nitrosylation mutant lines used in this study. Levels of S-Nitrosothiol (SNO) and pathogen susceptibility as know by fungal and bacterial studies are indicated. WRT = with respect to.

Mutant line	Level of SNO	Pathogen susceptibility	Reference
gsnor1-3	high (WRT Col-0)	Susceptible	Feechan *et al.*,2005
gsnor1-3 R	low (WRT Col-0)	Resistant	Feechan *et al.*,2005
nox1	high (WRT Col-0)	Susceptible	He *et al.*, 2004
TRXh5(*nox1*)	low (WRT nox1)	Resistant	Kneeshaw *et al.*,2014

NO and SNO mutants, *nox1* and *gsnor1-3* respectively, displayed resistance to TuMV in comparison to Col-0 (Figure 3.3, 3.4). *Gsnor1-3* showed lower viral load and a low rate of infection at 7 dpi. Increase in viral spread at individual and population level was seen with progression of time. At 21 dpi, level and rate of viral infection in gsnor1-3 was comparable to WT. Viral infection were similar to WT in complementary line, *gsnor1-3R*. Additionally, *nox1* showed very low rate of infection throughout the 3-week period. While TRXh5(*nox1*), a *nox1* pathogen phenotype rescue mutant, displayed significantly higher rate of infection (Student's *t*-test, $p < 0.05$). However, the viral load in *nox1* was comparable *to* TRXh5(*nox1*) at all three time points. Taken together, this assay indicates the role of nitrosylation in viral resistance against TuMV.

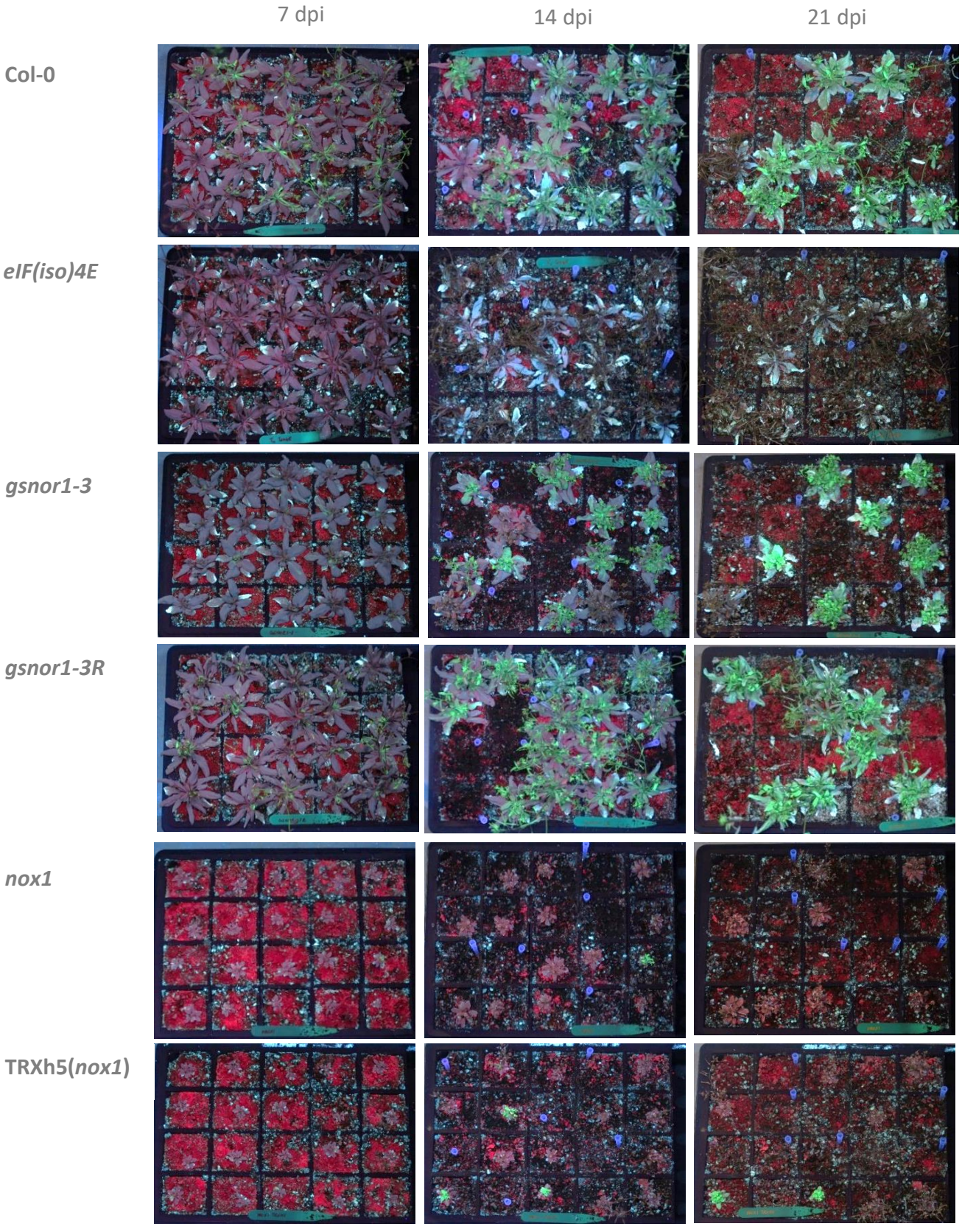
7 dpi
14 dpi
21 dpi
Col-0
eIF(iso)4E
gsnor1-3
gsnor1-3R
nox1
TRXh5(nox1)

Figure 3.3 Viral infection in *Arabidopsis* mutants with varying SNO levels. Col-0 and *eIF(iso)4E* were used as positive and negative control, respectively. Images show TuMV-GFP spread in Col-0, *eIF(iso)4E*, *gsnor1-3*, *gsnor1-3R*, *nox1*, TRXh5(*nox1*), under UV light at 7, 14 and 21 dpi.

3.2.3 Expression analysis of reductases

Denitrosylation is carried out by reductase enzymes such as GSNOR1 and TRXs. To test influence of viral infection on reductases i.e., GSNOR1 and TRXh5, we looked at their expression level 7, 14 and 21 dpi in Col-0 inoculated with TuMV-GFP. cDNA obtained from the samples collected during the TuMV susceptibility assay were used for this purpose.

TuMV inoculated Col-0 showed high level of viral load that increased with time, indicating successful viral infection (Figure 3.5B). GSNOR1 expression did not show variation over the time that the viral infection was monitored. TRXh5 expression, on the other hand increased with time. A 3- fold increase in expression was observed at 7 dpi which further increased to 6- fold at 21 dpi, implying need for TRXh5 based denitrosylation throughout viral infection.

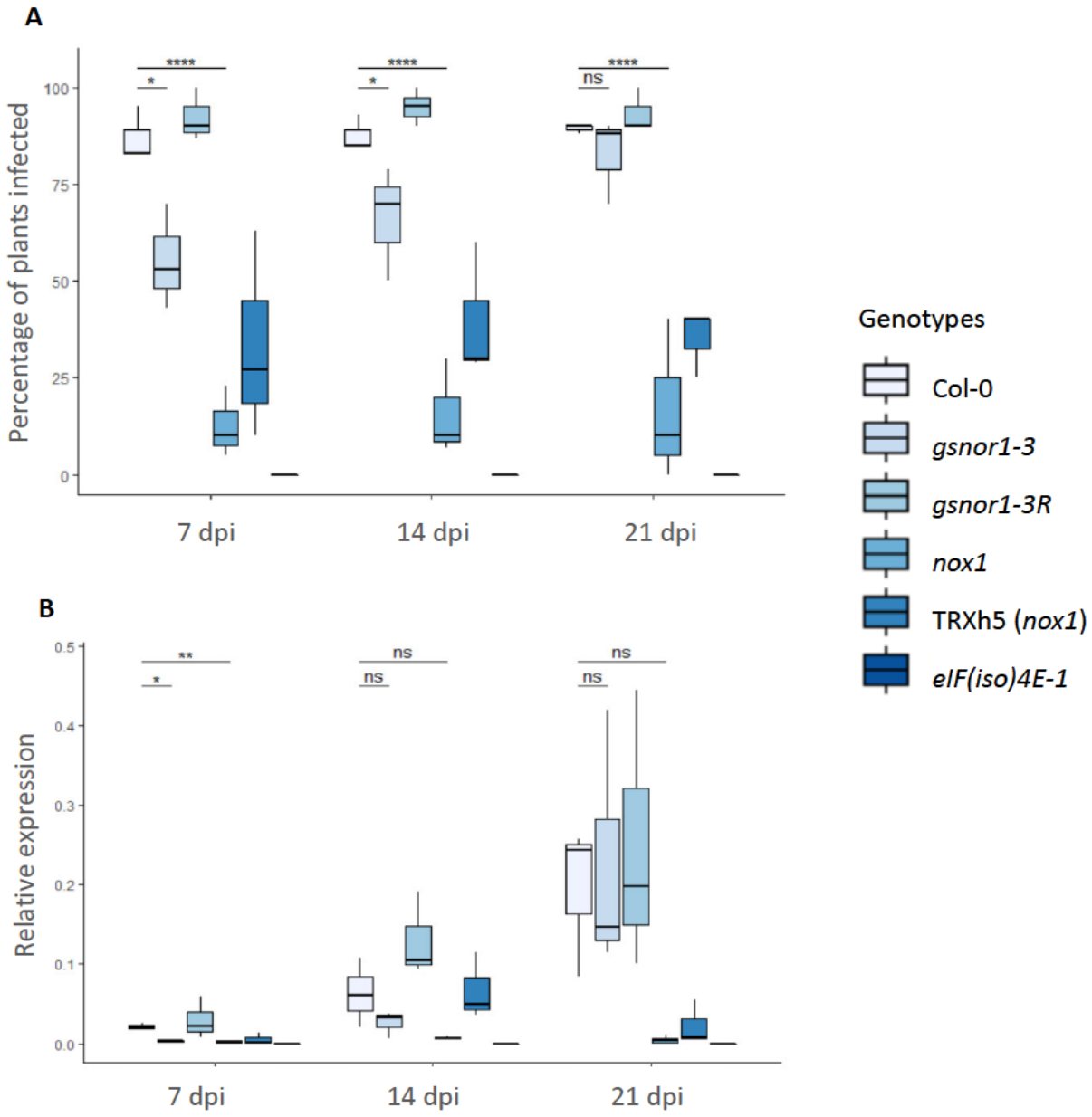

Figure 3.4 Viral infection in *Arabidopsis* mutants with varying SNO levels. (A) Percentage of plants infected (Number of plants infected/Number of plants inoculated*100) per genotype. (B) Quantification of viral load in each genotype by qRT-PCR. 6-10 plants were pooled together to form a sample. Viral RNA was measured by qPCR using TuMV CP primers. EF1a was used as reference gene. Error bars indicate SD of three biological replicates. Statistical analysis was carried out to

compare *gsnor1-3* and *nox1* with Col-0. ns, $p > 0.05$; *, $p < 0.05$; **, $p < 0.01$; ****, $p < 0.0001$ (Student's *t*-test).

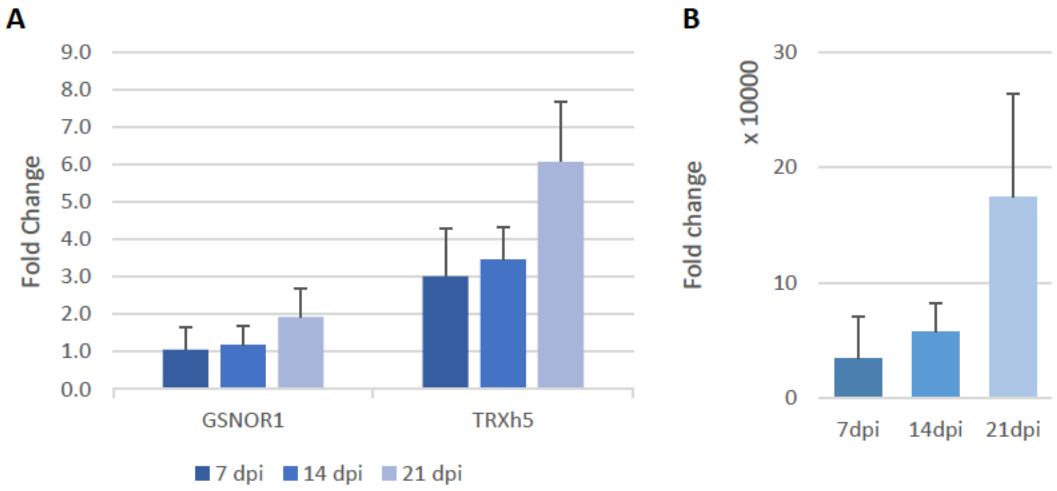

Figure 3.5 (A) Expression analysis of reductases in Col-0 upon TuMV infection. cDNA obtained from TuMV and mock inoculated Col-0 plants from TuMV susceptibility assay (Section 3.2.2) was subjected to qPCR using primers for *GSNOR1* and *TRXh5* to quantify mRNA level of these reductases. (B) TuMV CP primers were used to quantify viral load in the same samples. EF1a was used as reference gene. Transcript fold change shown here is relative to mock inoculated plants at corresponding time point. Error bars indicate SD of three biological replicates. Statistical analysis (Student's *t*-test) indicated that the expression of reductases did not vary significantly over the monitored period.

3.3 Discussion

In this study we demonstrate the role of S-nitrosylation in plant anti-viral response. Contrary to its role in bacterial and fungal pathogen response, increased SNO content slows onset of viral infections. Susceptibility assay carried out using NO and SNO *Arabidopsis* mutants (Figure 3.3, 3.4) showed lower viral infection in plants with higher SNO levels, while complemented mutants with lower SNO showed higher viral infection. The observed disease phenotype could be a result of molecular and/or physiological differences between the mutants and wild-type (WT) plants.

Both *gsnor1-3* and *nox1* have a well-defined morphological phenotype indicating abnormal growth and development (Figure 3.6). *Gsnor1-3* displays a semi-dwarf, bushy phenotype with reduced fertility (Chen *et al.*, 2009). *Nox1* plants are small in size with reticulated pale green leaves (He *et al.*, 2004). These morphological features could be a contributing factor in viral resistance seen in this study. Low viral infection at population level in *nox1* could be due to small leaf surface area resulting in ineffective rub inoculation. Small leaf size makes it harder to hold the leaf which in turn leads to inconsistency in rub inoculation, causing successful inoculation in some plants and not others. However, it is not the only factor influencing resistance as TRXh5(*nox1*) plants with complementary disease phenotype (against bacterial infections, Kneeshaw *et al.*, 2014) but same morphological phenotype to *nox1*, displays higher viral infection.

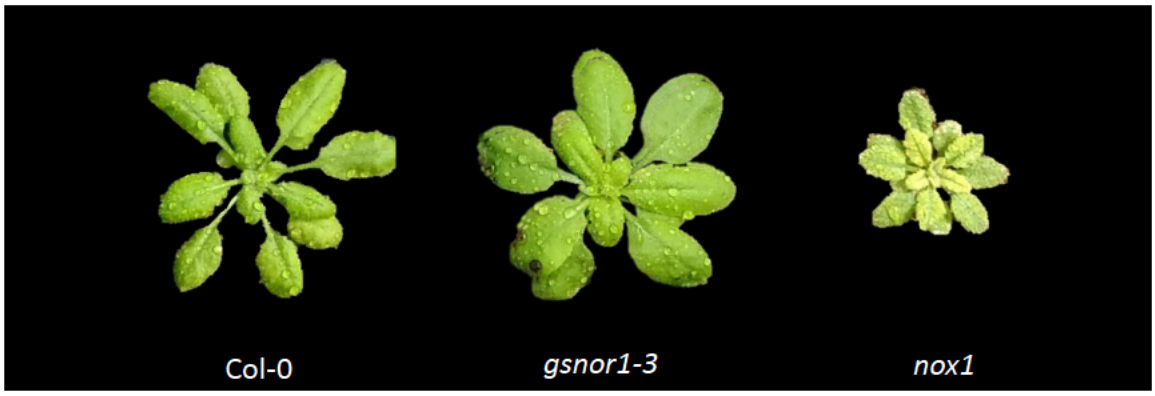

Figure 3.6 Representative images of Col-0, *gsnor1-3* and *nox1* to emphasize the morphological difference between WT and SNO mutants. Plants were grown in long day conditions (16hr/8hr light/dark) at 21°C. Due to slower development, *nox1* (5-week-old) was sown a week prior to Col-0 and *gsnor1-3* (4-week-old).

A large number of proteins have shown to be nitrosylated in *gsnor1*-3. These proteins cover a wide variety of biological functions such as metabolism, cell organization, biotic and abiotic stress and signal transduction (Hu *et al.*, 2015). We hypothesize that S-nitrosylation of either a single or a set of host/viral proteins is responsible for the viral resistance observed in *gsnor1-3* and *nox1*. Post translational modifications have previously shown to play a role in plant viral infection. Phosphorylation of Potato virus A (PVA) coat protein by host kinases strongly inhibited its RNA binding activity, suggesting regulation of formation/stability of viral ribonucleoproteins (Ivanov *et al.*, 2001). Later, protein kinase CK2 was identified as the enzyme responsible for PVA CP phosphorylation. Mutation of a major CK2 phosphorylation site in PVA CP lead to loss of viral infectivity (Ivanov *et al.*, 2003). Sumoylation of TuMV NIb is reported to promote TuMV infection by enhancing viral

replication and suppressing host antiviral response (Cheng *et al.*, 2017). Ubiquitylation of AGO1, a component of RNA silencing pathway, promotes its degradation via autophagy, presumably impairing RNA-based anti-viral immunity (Derrien et al., 2012). Another component of RNAi pathway, DCL4, is shown to be redox regulated (Seta *et al.*, 2017).

Pathogen susceptibility in *gsnor1-3* and *nox1* plants against biotrophic pathogens is shown to be a result of compromised SA pathway (Yun *et al.*, 2016a). S-nitrosylation of NPR1, SA master-regulator, prevents its nuclear localization resulting in lack of SA-dependent gene regulation. Additionally, SA has shown to trigger resistance at different phases of viral infection – viral replication and movement (Singh *et al.*, 2004). Therefore, it is particularly interesting that the plants with a comprised SA pathway can still display viral resistance. This implies involvement of a factor/pathway which is not regulated by SA but is either directly or indirectly regulated by S-nitrosylation. Double mutants such as *gsnor1-3nagH* or *gsnor1-3npr1*, could help understand involvement of SA pathway in anti-viral response seen in *gsnor1-3.*

Expression analysis of reductases GSNOR1 and TRXh5, reveal that GSNOR1 expression is not influenced by viral infection, while that of TRXh5 is. These two reductases are known to be involved in denitrosylation of different sets of proteins. TRXh5 selectively denitrosylate protein-SNO derived from free NO but not GSNO (Kneeshaw *et al.*, 2014). This is further demonstrated in this study. TuMV inoculated *nox1* plants with overexpressed TRXh5 i.e TRXh5(*nox1*) showed higher viral

susceptibility than *nox1* (Figure 3.3G). While *gsnor1-3* plants with overexpressed TRXh5 showed similar level of susceptibility as *gsnor1-3* (35-38% infection rate at 7dpi, data not shown). Therefore, the nitrosylation resulting in increased viral resistance was eliminated by TRXH5 based denitrosylation in *nox1* but not in *gsnor1-3*. This data suggests that protein-SNO(s) that is responsible for S-nitrosylation based anti-viral response is regulated by both TRXh5 and GSNOR1, as seen with *P. syringae* infection (Kneeshaw *et al.*, 2014).

Multiple avenues were considered to get a better understanding of the molecular mechanism of S-nitrosylation based delayed onset of viral infection. S-nitrosylation could regulate both viral and host proteins. S-nitrosylation of viral proteins might be responsible for a slow onset of infection possibly due to reduced/partially compromised function. Components of RNAi, a prominent anti-viral mechanism employed in plants, may be S-nitrosylated resulting in viral resistance. Multiple host proteins involved in spread of viral infection could be S-nitrosylated leading to a slower spread of pathogen. It could be one of these factors or a combination of all of them in addition to morphological factors. These possibilities are explored in the future chapters.

Chapter 4: TuMV replication and short distance movement are not impaired in gsnor1-3 plants.

4.1 Introduction

Virus infection is a multistep process that includes entry into plant cells, disassembly of virion to release viral genome, translation of viral proteins, replication of viral nucleic acid, assembly of progeny virions, cell-to-cell movement, and systemic movement (previously discussed in section 1.4.2). Successful implementation of each of these steps requires compatible host factors. Unavailability of these virus compatible host factors gives rise to resistance in plants. Multiple host factors have been identified that confer the plant with either full or partial resistance (Garcia-Ruiz, 2018). Hampered interaction of TuMV Vpg with eIF(iso)4E, host translation initiation factor, confers *Arabidopsis* with full resistance (Pyott *et al.*, 2016). While ineffective interaction between TuMV Vpg and host Potyvirus VPg-interacting protein (PVIP) results in reduced disease symptoms, giving rise to partial resistance (Dunoyer *et al.*, 2004). Similarly, unavailability of host plasma membrane protein PCaP1 for interaction with TuMV P3N-PIPO, led to reduced viral accumulation, fewer symptoms and localized viral infection sites (Vijayapalani *et al.*, 2012). In addition to these individual factors, TuMV also makes use of host cellular architecture such as the endoplasmic reticulum, chloroplast, plasmodesmata, for replication and for intra and inter cellular movement (Ivanov *et al.*, 2014).

Plasmodesmata (PD) (Figure 4.1) are cytoplasmic channels that connect neighbouring plant cells and facilitate cell-to-cell communication. PD allow transport of variety of substances, ranging from small solutes to large protein and RNA complexes such as viral genomes (Roberts and Oparka, 2003). Primary PDs are formed during cell division, by the entrapment of the endoplasmic reticulum in the developing cell plate, resulting in the formation of a cytoplasmic pore known as the cytoplasmic sleeve (Robards and Lucas, 1990). Actin filaments and myosin-like proteins along with the proteinaceous spoke-like projections localized within the cytoplasmic sleeve are thought to create nanochannels of varying size (White *et al.*, 1994; Radford and White, 1998). Callose, a β- 1,3-glucan polymer, appears to act as a structural element and has also been shown to regulate PD permeability (Radford *et al.*, 1998).

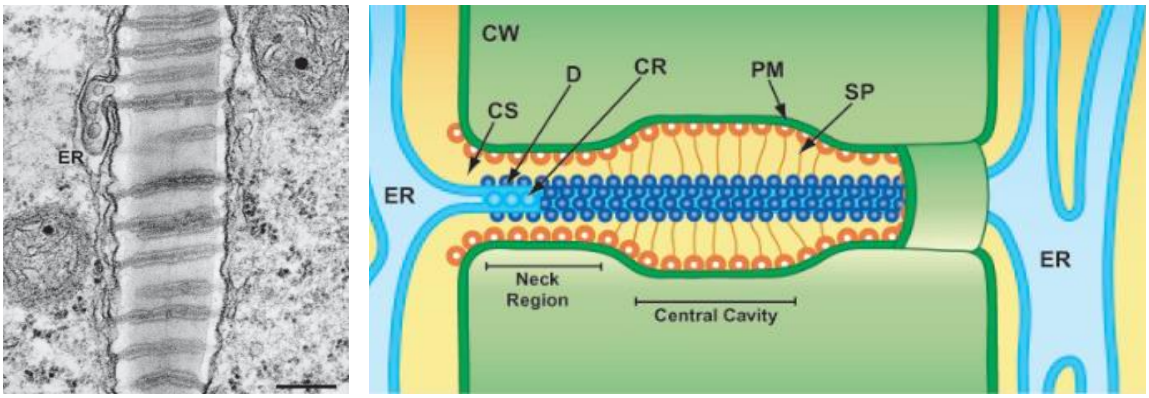

Figure 4.1 (A) Electron microscopy image of longitudinal section of simple PD. Bar = 200 nm. (B) Schematic model of simple plasmodesmata. ER, endoplasmic reticulum; CW, cell wall; CS, cytoplasmic sleeve; D, desmotubule; CR, central rod; PM, plasma membrane; SP, spoke-like extensions; PMP, plasma membrane-embedded proteins; DP, desmotubule-embedded proteins. (Roberts and Oparka, 2003)

The number of PD can change as the cell develops. In some cases, the number of PD can decrease. For example, during guard cell maturation, PD undergo disintegration as part of cell differentiation process (Palevitz and Hepler, 1985). In other cases, the number of PD increases as the cell expands. The PD formed post cell division are known as secondary PD (Ehlers and Kollmann, 2001). The exact molecular mechanism by which these are formed remains uncovered. However, cell wall degrading enzymes and ER binding proteins are speculated to be involved in the process (Burch-Smith and Zambryski, 2012). Additionally, some of the cues that trigger formation of secondary PD have been identified. The triggers include floral transition, cytokinin and salicylic acid (Ormenese *et al.*, 2000, 2006; Fitzgibbon *et al.*, 2013). Both primary and secondary PD start out as simple structure i.e., single pore traversing the cell wall. They later form complex branched structures either by intrinsic branching or by fusion with neighbouring PD (Roberts and Oparka, 2003).

Susceptibility assay in chapter 3 pointed towards slower onset of viral infection in plants with higher SNO level. Lower infectivity can be explained by either lower replication rate of TuMV in infected cells or reduced viral spread - local and systemic. In this chapter we explore viral replication and cell to cell movement in plants with increased SNO content.

Nox1 has a low rate of infection when compared to *gsnor1-3* (Figure 3.3G). However, it difficult to determine if the low infection rate is due to a physiological response against virus or ineffective rub inoculation owing to small leaf size. We lean more towards the latter as the infection rate in TRXh5(*nox1*), though higher than

nox1, is still quite low (Figure 3.4A). *Gsnor1-3*, on the other hand is easier to rub inoculate, making it a more reliable study. Additionally, it also displays an interesting pattern of infection i.e., low rate of infection at 7 dpi which increases to reach similar rate as that of Col-0 at 21dpi. Therefore, we focus on *gsnor1-3* mutants to better understand S-nitrosylation based delay in anti-viral response.

4.2 Results

4.2.1 Assessment of viral replication rate via protoplast assay

Protoplast assay was carried out to investigate the influence of S-nitrosylation on viral replication rate. 4-week-old Col-0 and gsnor1-3 plants were used to isolate protoplast as described in section 2.11. The protoplasts were then transfected with TuMV-GFP//mCherry plasmid (Cui *et al.*, 2017). Transfected protoplasts were monitored for 3 days with periodic sample collection for quantitative analysis by qPCR (Figure 4.2).

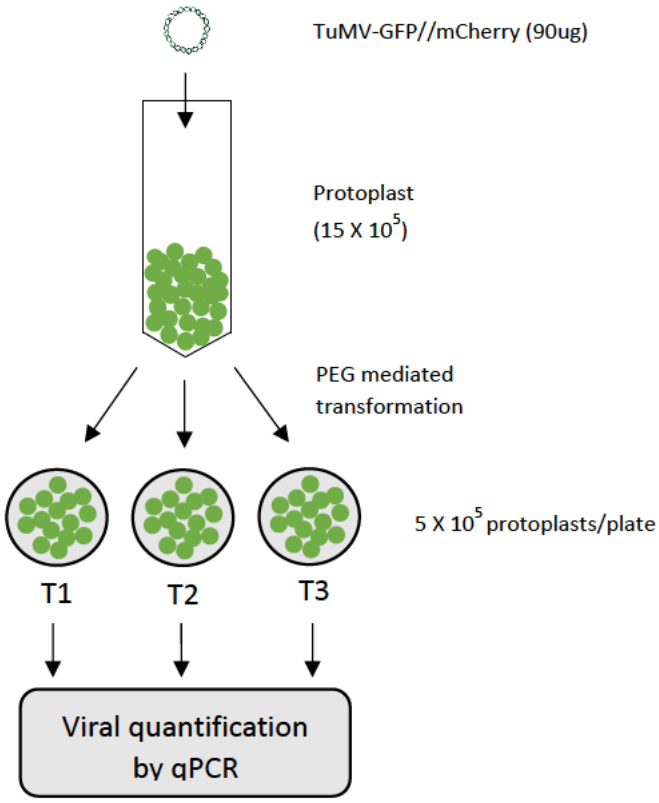

Figure 4.2 Schematic diagram of protoplast assay to assess viral replication rate. Isolated protoplasts ($15*10^5$) were transfected with TuMV-GFP//mCherry plasmid in a 15ml tube. Transfected protoplasts were transferred to petri dishes (35mm

diameter) such that each plate had a concentration of $5*10^5$, for storage till sample collection. RNA extracted from the samples was used to quantify viral load via qPCR.

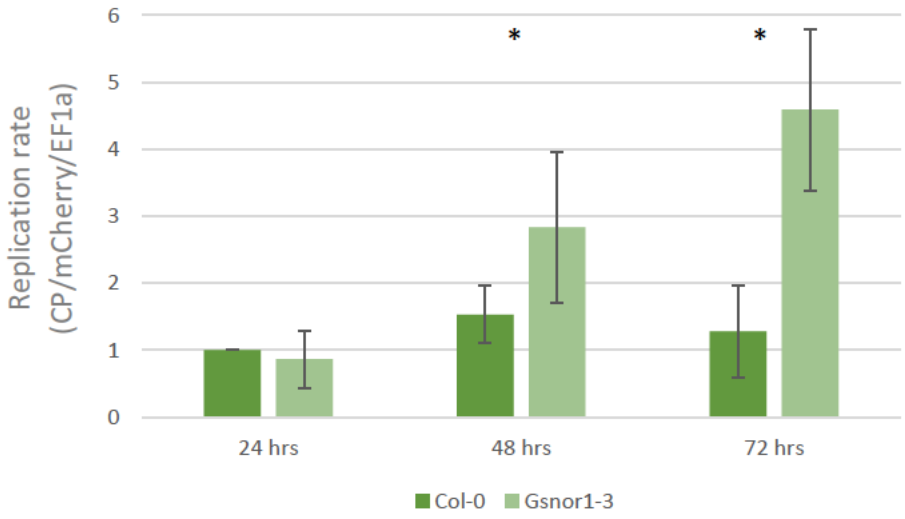

Figure 4.3 Viral replication rate in Col-0 and *gsnor1-3.* Protoplasts transfected with TuMV-GFP//mCherry plasmid were collected 24, 48- and 72-hours post-transfection. Viral replication rate was calculated by normalizing TuMV-GFP expression levels measured by qPCR to mCherry transcript levels. EF1a was used as reference gene. Bars here represent the arithmetic mean of 5 biological replicates ± SD and data is plotted relative to the mean of Col-0 24 hrs samples. *, $p < 0.05$ (Student's *t*-test).

Plasmid used for transfection i.e., TuMV-GFP//mCherry, allowed co expression of TuMV-GFP and mCherry from independent gene expression cassette located on the same plasmid backbone. This feature was used to normalize the viral expression level with mCherry expression level to account for viral RNA expression from the plasmid. Normalized quantification of viral RNA would then give the viral replication rate within a transfected cell.

Protoplast assay revealed that viral replication rate in gsnor1-3 was positively influenced by S-nitrosylation. Viral replication rate was similar 24 hours post transfection. However, significant difference in viral replication rate in favour of *gsnor1-3* was observed with progression of time i.e., 48 and 72 hours post transfection (Figure 4.3). This data indicates that viral replication rate in gsnor1-3 is not hampered as we had initially hypothesized.

Maintenance of protoplast for 72 hours after transfection posed a problem. Contamination was observed in samples collection at third time point i.e. 72 hours, in some experimental replicates. However, careful examination of cell viability data obtained using fluorescein diacetate which stains only live cells, and qPCR data, indicated that contamination did not influence the calculated viral replication rate.

4.2.2 Evaluation of plasmodesmata

Plasmodesmata (PD) play a crucial role in viral cell to cell movement and can be considered as a gateway to spread of viral infection. Viral proteins can increase PD permeability to allow the passage of virion or viral RNA complexes to move to the neighbouring cells (Wei *et al.*, 2010). Reduced PD count would then slow down viral movement to the adjoining cells. To test this hypothesis, we looked at number of plasmodesmata in Col-0 and *gsnor1-3* plants.

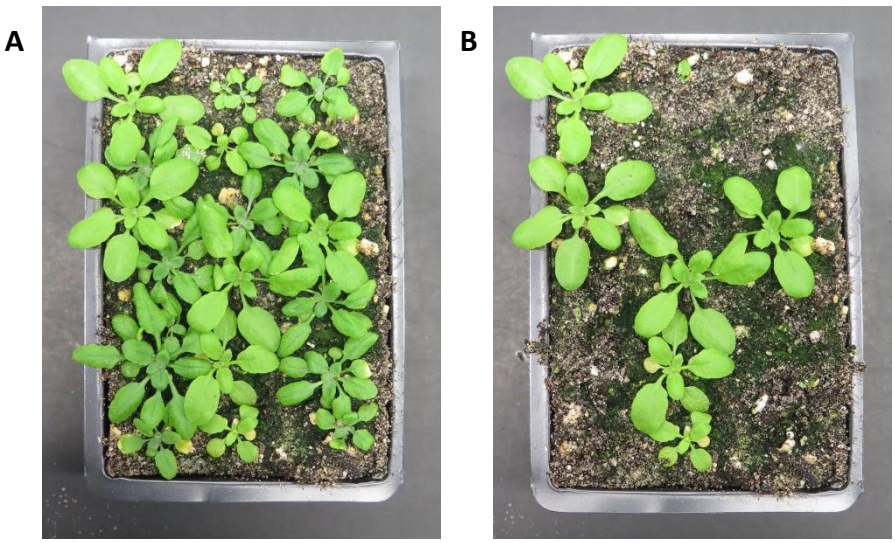

Figure 4.4 Screening F2 generation of *gsnor1-3* X PD. Two hundred F2_gPD seeds were sown individually (A) and screened for *gsnor1-3* phenotype at 3-week stage. Plants without *gsnor1-3* phenotype were weeded out such that only plants homozygous for *gsnor1-3* remained (B). Above pictures are representative and show a single pot, 12 such pots were monitored.

Plants that allowed fluorescent visualization of simple and complex PD were used to calculate PD count i.e., number of PD/100um Plasma membrane (PM). Plasmodesmata Localised Protein1 (PDLP1) fused with mRFP was used to label simple and complex PDs, and movement protein of potato leafroll virus (MP17) fused with GFP was used to label complex PDs (Fitzgibbon *et al.*, 2013). The transgenes for each of the PD localising protein- reporter units were independent and were driven by 35S promoter in Col-0 background in PDLP1 mRFP X MP17 GFP line (referred to as PD line in this study) used here. Confocal images of leaves from PD line were analysed to calculate number of PD/100um PM (PD count) for Col-0. To calculate PD count for gsnor1-3, PD line was crossed with gsnor1-3 (*gsnor1-3* X PD) and the resulting F2

generation was analysed. F2 generation seeds of *gsnor1-3* X PD (F2_gPD) were sown individually and monitored for *gsnor1-3* phenotype (Figure 4.4). *Gsnor1-3* phenotype is recessive and therefore only seen in homozygous condition. Plants with *gsnor1-3* phenotype were further checked for presence of both GFP and mRFP reporters. Such plants were then used to attain PD count for *gsnor1-3*.

The reporter expression in F2_gPD plants with both reporters, could arise from either a homozygous or a heterozygous genotype i.e. GxRy (G =GFP gene , g = no GFP gene, R=mRFP gene, r =no mRFP gene, x= G or g, y= R or r). Considering the reporters are expressed constitutively under 35S promoter it is unlikely that there would be a difference in PD labelling between the two genotypes. To verify this, lines homozygous and heterozygous for PD reporters in Col-0 background were compared for PD labelling. Homozygous PD line was crossed with Col-0 to obtain F1 plants that are heterozygous for both reporters. The heterozygous nature of the plants was confirmed by analysing progeny (F2) segregation ratio for GFP using fluorescent microscope. The F2 generation followed Mendelian 3:1 segregation ratio for GFP indicating successful crossing (Col-0 X PD) resulting in heterozygous F1. Analysis of PD count for plants homozygous and heterozygous for PD reporters suggests that the zygosity of reporter did not affect PD labelling (Figure 4.5E). This allowed us to use F2_gPD plants fulfilling aforementioned criteria irrespective of their zygosity to calculate PD count for *gsnor1-3*. Analysing PD in gsnor1-3 background revealed that the number of PD per 100um of plasma membrane (PM) is significantly lower in *gsnor1-3* than Col-0. This is true for both leaf 4 and leaf 7 that were analysed (Figure

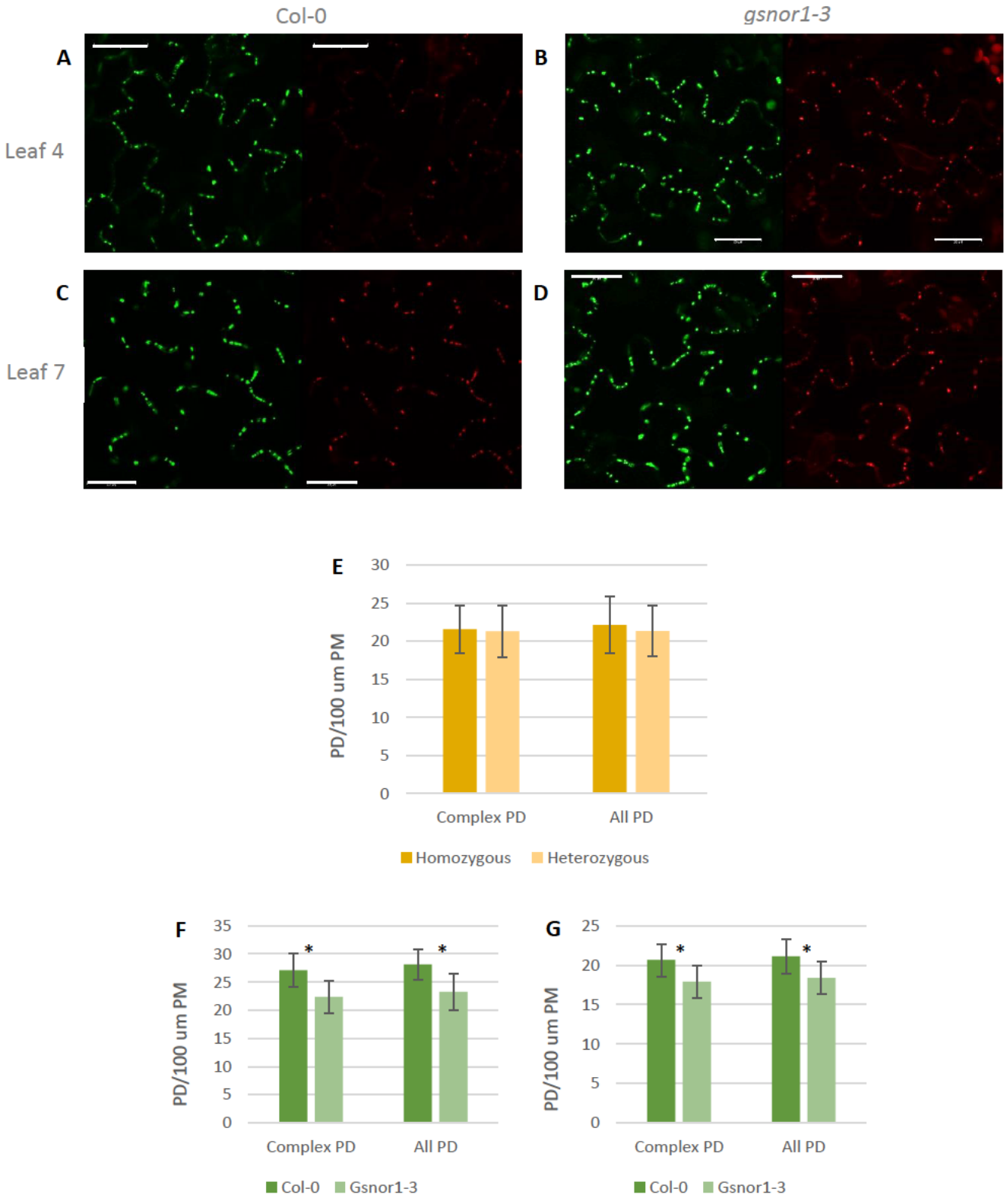

Figure 4.5 Evaluation of plasmodesmata. (A, B) Representative confocal images of the PD labelling in leaf 4 in Col-0 (A) and *gsnor1-3* (B). (C, D) Representative confocal

images of the PD labelling in leaf 7 in Col-0 (C) and *gsnor1-3* (D). First half of every image shows complex PD tagged by GFP; second half shows all PD tagged by mRFP. Bar = 20μM (E) Comparing efficiency of PD labelling in PD reporter lines with varying zygosity (homozygous vs heterozygous). Leaf 4 from 4-week-old Col-0 which are homozygous or heterozygous for PD reporter (mRFP for all PD, GFP for complex PD) were analysed using confocal microscopy. Resulting images were analysed by Image J. Three regions were analysed per leaf and averaged to obtain PD count for a leaf. Error bars indicate SD of four replicates. (F, G) PD count for leaf 4 (F) and leaf 7 (G) of Col-0 and *gsnor1-3*. Error bars indicate SD of eight replicates. *, $p < 0.05$ (Student's *t*-test).

4.5F, G). Lower number of PD in *gsnor1-3* could be one of the contributing factors for slow viral onset in this genotype.

4.2.3 Cell to Cell movement assay

Once established within the entry cell, viruses move to the adjoining cells via plasmodesmata to initiate spread of infection. In this assay we monitor viral cell to cell movement by analysing the initial foci of infection. To achieve this 4-week-old Col-0 and *gsnor1-3* plants were bombarded with TuMV-GFP//mCherry plasmid (Cui *et al.*, 2017). The inoculated leaves were checked for infection foci (GFP expressing area) using confocal microscope. Different sets of leaves were imaged 4, 5 and 6 dpi and area of viral spread was measured with Image J.

Analysis of infection at early stages shows that there is no significant difference in area of infection foci between Col-0 and *gsnor1-3*, at any of the measured time points (Figure 4.6D). However, the violin plots show that the data distribution between the two genotypes is not the same. *Gsnor1-3* has higher number of smaller foci while foci size in Col-0 is more uniformly distributed at 4 and 5 dpi. The lack of statistical significance in infection foci area between the two genotypes indicates that the cell-to-cell movement of virus between the two is similar.

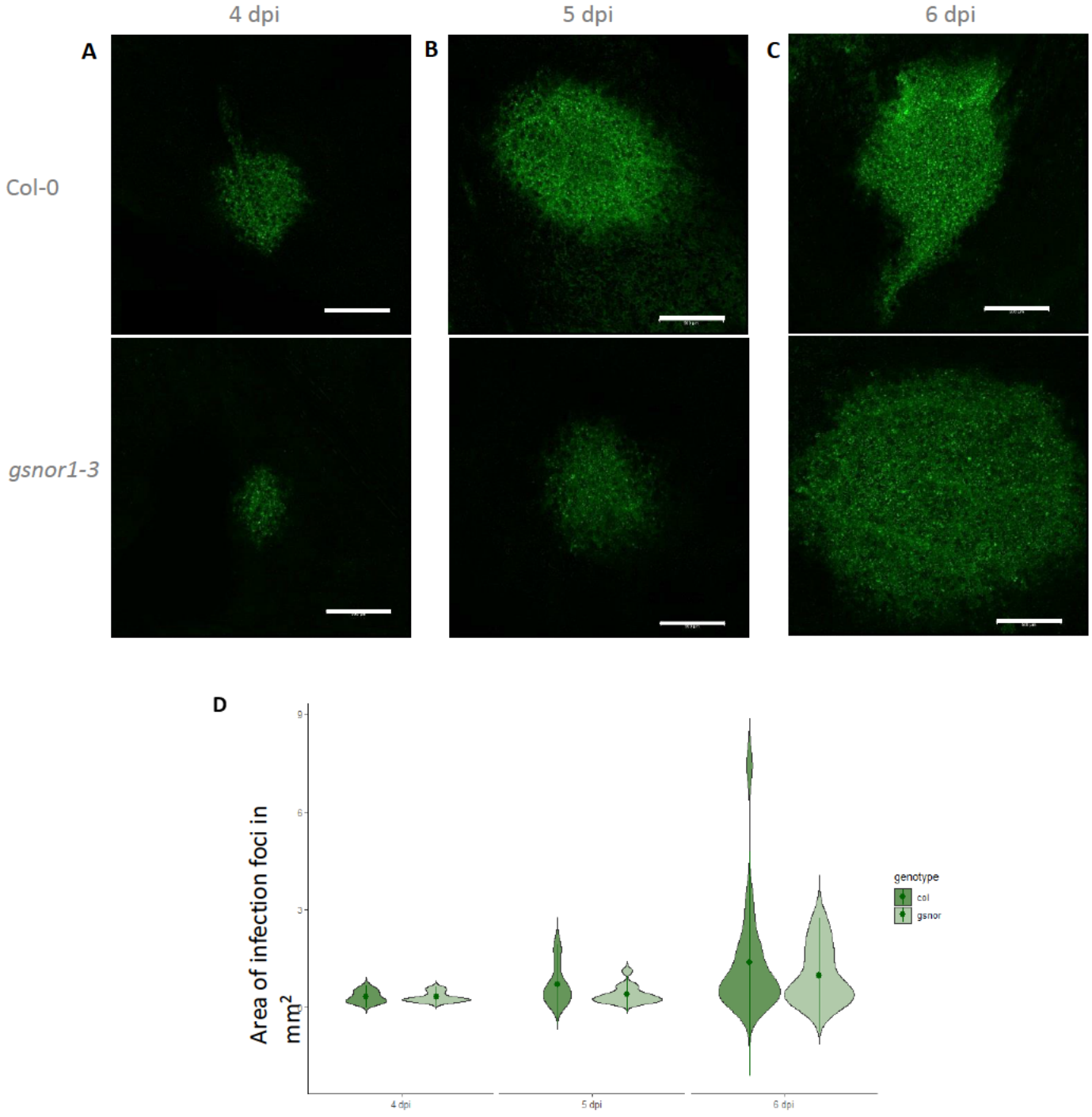

Figure 4.6 Viral cell to cell movement analysis. Leaves of 4-week-old Col-0 and *gsnor1-3* were bombarded with TuMV-GFP//mCherry plasmid using gene gun and monitored from 4 to 6 dpi. Bombarded leaves were inspected using confocal microscope for infection foci i.e., region expressing GFP. A, B, C are representative

images for TuMV infection foci seen in Col-0and *gsnor1-3* at 4, 5 and 6 dpi respectively. Bar = 0.5mm. Confocal images were then analysed to calculate area of infection foci using image J. (D) Violin plot displaying the distribution of area of infection in Col-0 and *gsnor1-3* at 4 (n=10), 5 (n= 13) and 6 dpi (n= 19). n is number of foci. Dot within the plot indicates mean, line indicates SD.

4.3. Discussion

Reduced viral infection in plants with increased SNO levels indicates towards hinderance in initial steps of viral infection i.e., viral replication and cell to cell movement. To identify the rate limiting step in viral infection in *gsnor1-3* we looked at viral replication rate, plasmodesmata number and cell to cell movement rate.

We hypothesized that slow onset of TuMV infection in *gsnor1-3* could be attributed to reduced replication. One of the major interfering factors in viral replication is the anti-viral RNA silencing pathway. A hyperactive anti-viral immune response, possibly due to nitrosylation, could explain reduced population and individual level infection. Spread of infection at later time point may be due the virus's ability to suppress RNAi components. To test this, we carried out protoplast assay to measure viral replication rate in *gsnor1-3* in comparison to Col-0. Contrary to expectation, viral replication rate was significantly higher in *gsnor1-3* protoplasts, 48 and 72 hours post transfection, when compared to wild type. This suggests that viral RNA synthesis is not affected in *gsnor1-3*. Similar results were seen in *PcaP1* mutant which displayed high replication rate in protoplasts despite of lower viral accumulation and localized infection in plants (Vijayapalani *et al.*, 2012). This was attributed to the localization of viral RNA in protoplasts. *PcaP1* mutants were speculated to accumulate less viral RNA at the periphery due to disrupted transport. Thereby allowing viral RNA to persist near replication factories for further rounds of replication. This could be the case in *gsnor1-3* mutants as well, which would then indicate that viral resistance observed in *gsnor1-3* plants is likely to be associated with viral movement rather than viral replication.

Protoplasts provide a single cell system to study viral replication without any interference from neighbouring cells. However, they do not provide a true representation of what happens in a complex multicellular plant. On isolation protoplast undergo reprogramming and display altered metabolism and stress responses (Xiao *et al.*, 2012). Enzymatic isolation of protoplasts have shown to disrupt cellular redox homeostasis and is associated with ROS generation (Ishii, 1987). Therefore, the replication rate obtained from protoplast assay might not be a true representation of what happens in the plant. It might be more informative to check viral replication in Col-0 protoplast with and without NO donor.

Large scale identification of S-nitrosylated proteins in Col-0 and *gsnor1-3* (Hu *et al.*, 2015) indicated nitrosylation of eIF(iso)4E in Col-0 but not in *gsnor1-3*. Lack of nitrosylation of eIF(iso)4E in *gsnor1-3* could be responsible for higher replication rate observed in the genotype. Additionally, post translational modification of viral proteins has shown to influence viral replication. Sumoylation of TuMV NIb promoted viral infection (Cheng *et al.*, 2017). Therefore, higher replication due to possible nitrosylation of viral proteins cannot be ignored.

Next, we focussed on the following step in infection – cell to cell movement, by analysing PD and initial infection foci. Since gsnor1-3 plants have distinct morphologically and physiological features (Kwon *et al.*, 2012), we looked at number of PD (PD number) in this genotype. Variation in PD number compared to wild type would indicate possible effect on viral cell to cell movement. To test this, as described in section 4.2.2, mRFP was used to tag all PD, while GFP was used to tag complex PD.

The tagged leaves were then imaged using confocal microscopy. Analysis of confocal images indicated that both GFP and mRFP tags identified same number of PD. This is likely due to non-specific cell wall labelling with mRFP in older leaves as seen previously in PD line (Fitzgibbon *et al.*, 2013). Since complex PDs supersede simple PDs, it might be reasonable here to just look at complex PDs tagged by GFP. Number of complex PD per 100um PM were significantly lower in *gsnor1-3* when compared to WT in both leaf 4 and 7 (Figure 4.5F, G). This host feature could slow down the spread of viral infection into neighbouring cells. However, measuring foci of infection at early time point (Figure 4.6D) indicated otherwise. There was no difference in area of infection foci in *gsnor1-3* and Col-0. This may be due to difference in permeability of PD in the two genotypes.

PD permeability has shown to be influenced by environmental factors such as hormones, redox state, calcium flux. Genetic screens aimed at screening plants with modified SEL, identified ISE1, a mitochondrion-localized DEAD-box RNA helicase; ISE2, a chloroplast-localized DEVH-box RNA helicase and TRX-m3, chloroplast-localized antioxidant thioredoxin m3, all involved in redox regulation (Sager and Lee, 2014). ISE1 silencing led to increased ROS production and increased intracellular permeability (Stonebloom *et al.*, 2009, 2012). Antioxidant TRX-m3 knockout mutant *gat1* with high ROS, displayed decreased trafficking via PD (Benitez-Alfonso *et al.*, 2009). Both these studies indicate that oxidative state influence PD permeability. In addition to ROS, SA was also shown to regulate PD trafficking via plasmodesmata- located protein 5 (PDLP5), negative regulator of PD permeability (Lee *et al.*, 2011). High SA concentration increased PDLP5 transcript levels which in

turn resulted in reduced PD trafficking. Defective SA pathway, therefore increased PD permeability (Lee *et al.*, 2011). It is therefore like that *gsnor1-3* which has an altered redox state as well as compromised SA pathway, regulates PD trafficking differently than Col-0. Additionally, PD structure could be modified in *gsnor1-3* by possible S-nitrosylation of PD structural proteins. This could also play a role in regulation of viral cell-to-cell movement via PD.

Area of infection foci suggests that the mechanism by which TuMV moves to neighbouring cell is not impaired. However, a few things need to be considered here. The method of delivery of viral genome into plant cells in cell movement assay (4.2.3) is different from that used in susceptibility assay (3.2.2). Former uses particle bombardment, while the latter uses rub inoculation. Particle bombardment with gold particles has shown to delivery desired DNA mostly into mesophyll cells (Hunold *et al.*, 1994). Rub inoculation on the other hand introduces viral particles into epidermal cells (Bennett, 1940). The form in which viral genome is delivered into these cells is also different in the two methods. Particle bombardment delivers plasmid carrying viral genome, while rub inoculation delivers virions i.e., viral genome bound to CP. Expression of viral genome under the control of 35S promoter in a plasmid is likely to be different from expression of viral genome from virions that requires disassembly and successful hijacking of the host machinery. Therefore, the time taken to establish viral RNA in the cell may vary depending on the source of viral genome, in turn effecting the time when cell-to-cell movement is achieved. Another factor to consider between the two methods is cellular damage made during the process of inoculation. We observed that particle bombardment caused lesser damage than rub inoculation.

Therefore, the rate of spread we notice when viral genome is delivered via particle bombardment might not be the same as that seen using rub inoculation.

Cell-to-cell movement assay used of TuMV-GFP//mCherry plasmid to differentiate primary and secondary infections. Reporter mCherry would be expressed only in cells that had the plasmid i.e., cells of viral entry while GFP expression would indicate movement of virus from the initial site (Cui *et al.*, 2017). Though the experiment design was elegant it could not be enforced in this study. Confocal analysis of leaves bombarded with TuMV-GFP//mCherry plasmid, did not show expression of mCherry at 4dpi, making it difficult to identify the site of initiation. Analysis of leaves at an earlier time point may have been more helpful in this regard. Lack of mCherry expression results in an unknown start point making it difficult to state if the secondary infection denoted by GFP expression is truly comparable. Using another system such as *N.benthamiana* with GSNOR mutation might make study of viral cell-to-cell movement easier. Larger leaf size, ease of agroinfiltration, make *N.benthamiana* an easier study when compared to *Arabidopsis.* In support of this, agroinfiltration of TuMV-GFP//mCherry plasmid in WT *N.benthamiana* leaves carried out to test the plasmid allowed detection of both primary and secondary infection foci.

Chapter 5: Delayed systemic movement contributes to increased TuMV resistance in gsnor1-3 plants.

5.1 Introduction

Plant vasculature consists of two conducting tissues - non-living xylem and living phloem. Xylem is involved in water and mineral conduction, while phloem transports sugars and macromolecules such as proteins, mRNA, phytohormones. Phloem comprises of companion cells (CCs), sieve elements (SEs), supporting bundle sheath (BS) and phloem parenchyma cells. Phloem transport occurs through SE, highly specialized anucleate cells that depend on CC for metabolic functions. The two cell types are connected by specialized branched PD known as plasmodesmata pore units (PPUs) that controls the transport within the phloem.

Viruses make use of the existing host systemic transport system i.e. vasculature to move systemically. On reaching phloem from the initial site of infection, viral cell to cell movement continues through phloem tissues – BS, vascular parenchyma, and CC, until sieve elements are reached. Once in sieve elements, viral transport is passive and follows the source-to-sink flow of phloem sap. This allows viruses to reach distant tissues quicky and spread infection to the entire plant. On reaching systemic tissue, cycle of replication and cell to cell movement continues (Wang and Zhou, 2016).

Phloem-specific resistance genes can effectively prevent viral systemic movement despite of successful replication and cell-to-cell movement. Phloem

associated Restricted TEV Movement 1 and 2 (RTM1/2), have been shown to play a role in restriction of potyviral long distance movement (Chisholm *et al.*, 2001). However, the molecular mechanism by which this is accomplished is not fully understood.

In chapter 4, we looked at initial stages of viral infection - viral replication and cell-to-cell movement, both of which were not hampered in *gsnor1-3*. This led to exploration of next stage of viral infection i.e. systemic movement. In this chapter, we demonstrate delayed systemic movement in *gsnor1-3* when compared to Col-0. We also explore the possible causes for the delay by looking at the means of systemic movement – plant vasculature system specifically its pattern and transport rate.

5.2 Results

5.2.1 Systemic movement assay

To explore possible variation in systemic movement between Col-0 and *gsnor1-3,* 4-week-old plants were infected with TuMV-GFP and monitored for 11 days. Inflorescence from infected plants was collected to check for viral level in systemic tissue. Difference in virus accumulation in systemic tissue i.e. inflorescence, would indicate variation in viral systemic movement.

24 plants per genotype were inoculated with TuMV-GFP. However, only the plants that showed signs of infection at 7 dpi were taken further. Since *gsnor1-3* has lower infection rate, number of plants used in the assay were determined by number of *gsnor1-3* plants infected at 7dpi. Inflorescence was collected from infected plants at 7, 9 and 11 dpi and processed to quantify the viral load via qPCR.

Careful observation of area of GFP in infected plants, indicated a slower spread of virus in *gsnor1-3* (Figure 5.1 A, B, C). This phenotypic observation was further confirmed by qRT-PCR. As expected, viral load increased in both genotypes with time. However, *gsnor1-3* displayed reduced viral load when compared to Col-0 at all measure time points, with significant difference at 7dpi. Taken together, the data suggests lower rate of TuMV systemic movement in *gsnor1-3*.

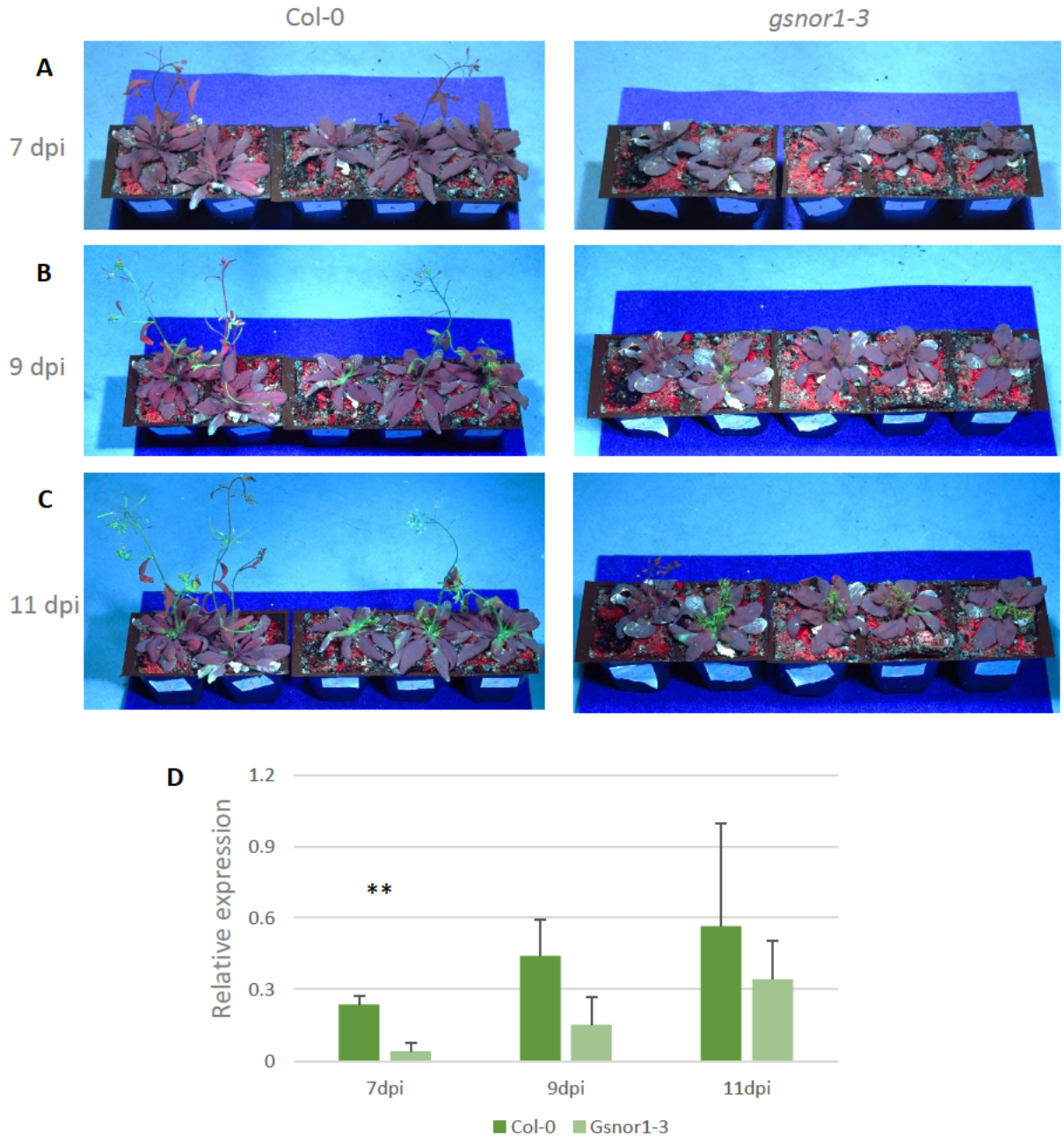

Figure 5.1 Systemic movement assay. Visual monitoring of viral spread in TuMV-GFP infected Col-0 and *gsnor1-3* at 7 dpi (A), 9dpi (B) and 11dpi (C). Plants were photographed under UV light to visualize GFP. (D) Analysis of viral load in systemic tissue (inflorescence) by qRT-PCR. Inflorescence from 2-3 infected plants were pooled together to form a single sample. Samples were processed to quantify expression of viral RNA by qPCR. EF1a was used as reference gene. Error bars indicate SD of three replicates. **, $p < 0.01$ (Student's *t*-test).

5.2.2 Venation pattern analysis

Long-distance viral movement occurs through plant vascular system. To gain insight in observed delay in systemic movement (Figure 5.1), we looked at vascular patterning in *gsnor1-3*. Leaf 4, 7 and 10 from 4-week-old Col-0 and gsnor1-3 were cleared and imaged using stereomicroscopy. The images were analysed using phenoVein software to obtain total vein length, vein density, areole area, and skeleton graph statistics (Bühler *et al.*, 2015). Data obtained from phenoVein is presented as graphs in figure 5.2.

Analysis of images and quantitative data from phenoVein revealed that, in both Col-0 and *gsnor1-3* the vascular pattern changes with age of the leaf. Newer leaves have a dense network of veins, while in older leaves the network becomes less dense (Figure 5.2A, D). Leaf 4 in both Col-0 and *gsnor1-3* displays similar venation pattern and areole (area bound by veins) size. However, Leaf 7 and leaf 10 show variations despite of similar leaf size in both genotypes (Figure 5.2C). Vein density and number of skeleton branching points were significantly lesser in *gsnor1-3* (Figure 5.2 A, D, E). In agreement with that, areolar size was significantly larger in *gsnor1-3* (Figure 5.2F). This data suggests that there is a variation in development of vascular system in *gsnor1-3* when compared to Col-0. This variation could be a contributing factor to slower viral systemic movement as it would take longer for virus to reach phloem.

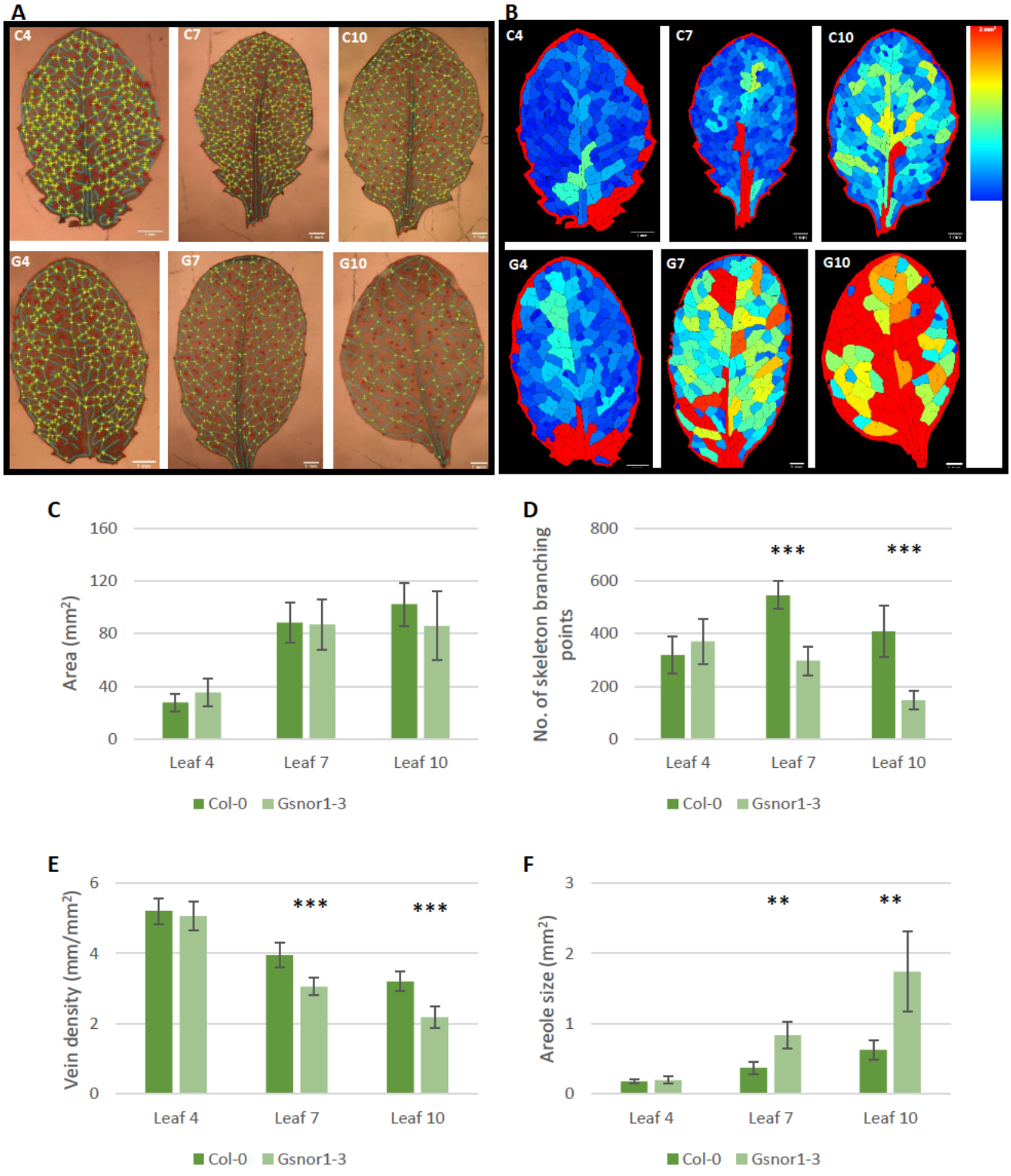

Figure 5.2 Venation pattern analysis in Col-0 and *gsnor1-3*. Leaf 4, leaf 7 and leaf 10 from 4-week-old plants were cleared, imaged and analysed. (A) Vascular pattern

observed in Col-0 and *gsnor1-3* leaves. C4, C7, C10 - leaf 4, 7 and 10 from Col-0; G4, G7, G10 - leaf 4, 7 and 10 from *gsnor1-3*, respectively. Teal lines represent veins, yellow crosses represent branching points, red crosses represent skeleton end points. Bar = 1mm. (B) Areole sizes observed in Col-0 and *gsnor1-3* leaves ranging from 0 to 2 $mm^{2.}$ Graphical representation of leaf area (C), skeleton branching points (D), Vein density (E), and areole size(F), obtained from phenoVein software for leaf 4, 7 and 10 in Col-0 and *gsnor1-3*. Error bars indicate SD of seven replicates. ***, $p < 0.001$; **, $p < 0.01$ (Student's *t*-test)

5.2.3 Phloem transport assay

In addition to vascular patterning, we also looked at phloem transport rate in *gsnor1-3.* We hypothesized that variation in rate of transport between Col-0 and *gnsor1-3* will affect the systemic movement of viruses. To test this, we monitored esculin translocation from cotyledons to true leaves in seedlings (Section 2.10). Esculin, a fluorescent coumarin glucoside, is a sucrose analog used to measure phloem transport rate (Knox *et al.*, 2018). Cotyledons were treated with the adjuvant Adigor to facilitate esculin loading. Esculin was added onto pre-treated cotyledons. Four hours post loading, exogenous esculin was washed off the cotyledon (Wash), while internalized esculin within the cotyledon and that translocated to true leaves was measured using a fluorometer. Fluorescence in terms of arbitrary unit (a.u) obtained from the fluorometer was proportional to esculin in the sample.

Preliminary attempts with phloem transport assay highlighted difference in surface area in 10-day old Col-0 and *gsnor1-3* seedlings. This was resolved by sowing *gsnor1*-3 two days before Col-0. Additionally, seedlings to be used for the assay were

photographed and images were used to measure seedling surface area using ImageJ. The assay was carried out only if there was no significant difference in seedling size between the two genotypes (Figure 5.3D).

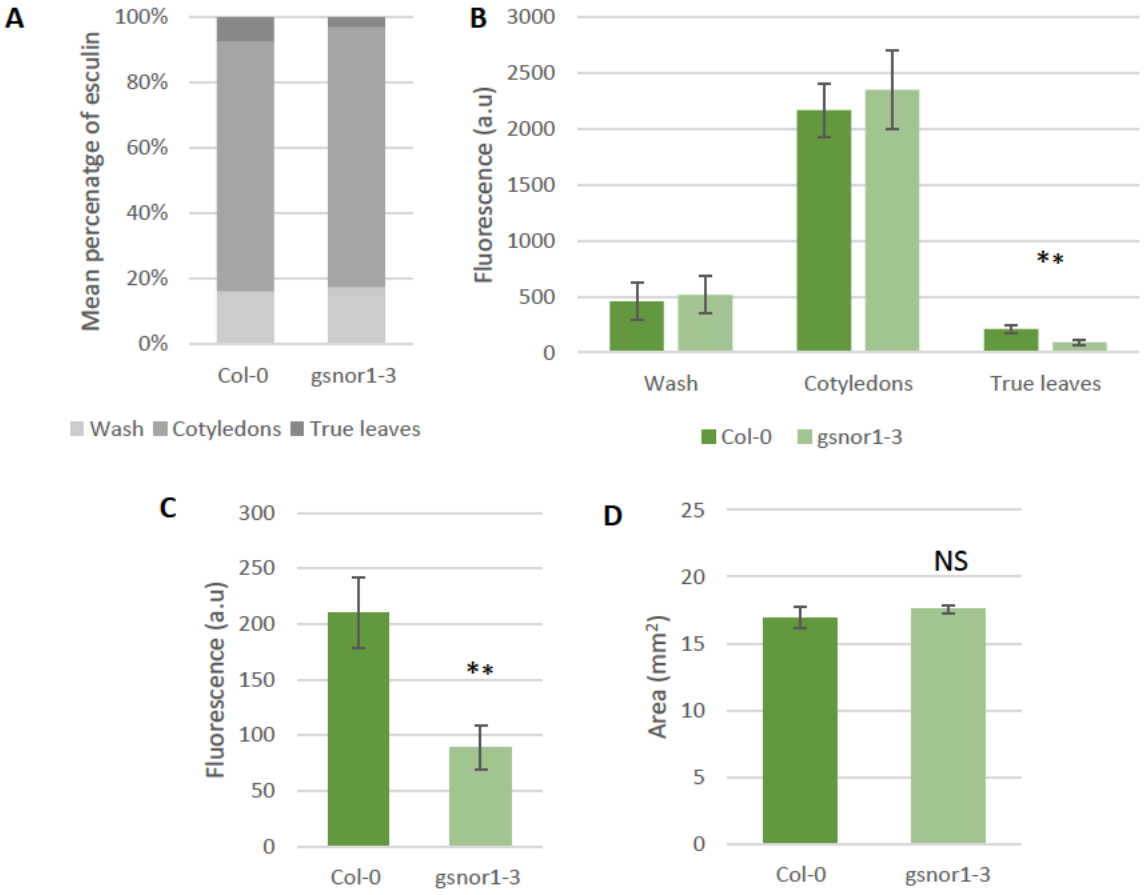

Figure 5.3 Phloem transport assay. Pre-treated cotyledons of 12-day old *gsnor1-3* seedlings and 10-day old Col-0 seedlings were treated with 9µg of esculin. Esculin in cotyledons (on surface and within) and true leaves was measure using fluorometer. 3 samples (5 seedlings /sample) were used per experiment. (A) Percentage of esculin in analysed fractions i.e. wash, cotyledons and true leaves (B) Esculin measured in analysed fractions by fluorometer. (C) Esculin in true leaves. (D) Measurement of Col-

0 and *gsnor1-3* seedling size. Error bars indicate SD of three replicates. **, $p < 0.01$; NS, not significant (Student's *t*-test).

Level of esculin that was washed off (16-17%) and that which remained (77-80%) in cotyledon (Figure 5.3 A, B) was similar in Col-0 and *gsnor1-3* seedlings. 7% of loaded esculin was found in true leave of Col-0 seedlings. While only 3% of loaded esculin was translocated to true leaves in gsnor1-3 seedlings (Figure 5.3A, C). Esculin measured in true leaves of *gsnor1-3* is significantly lower than that in Col-0 (Figure 5.3 C), suggesting lower phloem transport rate in *gsnor1-3*.

5.3 Discussion

Successful viral replication is followed by viral spread first to the neighbouring cell and then to the rest of the host. Viral cell to cell movement varies from systemic movement not just in the distance travelled but also mechanism used. Cell to cell movement relies on PD while systemic movement relies on plant vascular system. However, efficiency of cell-to-cell movement influences the long-distance transport of virus. Viruses move from cell to cell till they reach the vasculature, all the while replicating in each of the cells. Therefore, more the number of cells virus must move through to reach the phloem, longer it would take to establish systemic infection. Systemic movement assay and venation pattern analysis indicates this to be true in *gsnor1-3*. Slower systemic movement was observed in *gsnor1-3* when compared to Col-0 (Figure 5.1D), especially at an earlier time point i.e. 7 dpi. Further, analysis of venation pattern shed light on the possible reason. Larger areole size, lower vein density (veins/mm^2 leaf area) in *gsnor1-3* despite similar leaf area as Col-0, suggests (Figure 5.2) that virus would require to move longer distance in *gsnor1-3* when compared to Col-0 to reach vasculature. It may be necessary here to determine the number of cells within each areole to then confirm that virus must pass through more cells in *gsnor1-3* than in Col-0 to reach phloem.

Kawabe *et al*. demonstrated the role of s-nitrosylation in development of vasculature. The study was designed to identify novel regulators of Vascular-Related NAC Domain 7 (VND7), an inducer of xylem vessel cell differentiation, using a forward genetics approach (Kawabe *et al.*, 2018). It led to the identification of mutant seiv1, a suppressor of mutant for xylem vessel cell differentiation, which was later identified

as a novel mutant allele of GSNOR1. Venation pattern analysis carried out in this study using 7-day-old cotyledons (*seiv1* and *gsnor1-3*), showed abnormalities in vein formation in cotyledons, i.e. discontinuous venation, and the formation of vascular islands. This observation taken together with venation pattern analysis here (Section 5.2.2), suggests that the vascular tissue in *gsnor1-3* does not follow the normal development pattern as seen in Col-0. The underdeveloped pathway of systemic movement could explain the delay seen in spread of viral infection in *gsnor1-3*. Additionally TuMV is shown to move systemically through both xylem and phloem (Wan *et al.*, 2015), lack of differentiated xylem structures could also be a contributing factor in reduced viral movement.

Systemic viral movement occurs passively along the source-to-sink flow of photo assimilates through phloem (Hipper *et al.*, 2013). The rate of phloem transport would then determine the rate of systemic viral spread. In this study we have shown the phloem transport rate is significantly lower in *gsnor1-3* than in Col-0 (Figure 5.3C, p= 0.005). Reduced transport rate is likely to reduce viral spread in *gsnor1-3.*

Phloem transport rate is known to be influenced by concentration of sucrose; a major solute found in phloem sap. Sucrose concentration in turn is dependent on chlorophyll metabolism and photosynthesis, both of which are heavily regulated by S-nitrosylation (Hu *et al.*, 2015). Additionally, *gsnor1-3* displays reduced chlorophyll level and altered photosynthetic activity (Hu *et al.*, 2015). Taken together reduced phloem transport rate is presumably a result of regulation of photosynthesis by s-nitrosylation.

Mutant *gsnor1-3* displays a wide range of developmental defects such as severe bushiness, loss of apical dominance, shorter primary roots, fewer lateral roots, and shorter hypocotyls (Liu *et al.*, 2015). These features can in turn affect the source-sink dynamics (Schulz, 1994; Kebrom, 2017) in the *gsnor1-3* plants which could result in varied viral transport compared to Col-0. Moreover, *nox1* plants that do not display the aforementioned morphological features, show a similar pattern of viral spread as Col-0 (Figure 3.3), suggesting that *gsnor1-3* morphology could be a contributing factor in the slower viral spread. This visual observation needs to be confirmed via systemic movement assay in *nox1*. Additionally, mutants with similar morphology as *gsnor1-3* (bushy plant, underdeveloped vasculature) but unaffected in S-nitrosylation can be used to discern if the slower systemic movement in *gsnor1-3* is due to its morphology or an SNO-based anti-viral response.

To summarize, reduced systemic movement observed in *gsnor1-3* is due to the additive effect of multiple factors. Underdeveloped vasculature as indicated by venation pattern analysis, impaired xylem cell differentiation due to s-nitrosylated VND7, and reduced phloem transport rate, have been discussed here as few contributing factors. The likelihood of additional factors cannot be ignored.

Chapter 6: Is S-nitrosylation mediated anti-viral response broad-spectrum?

6.1 Introduction

Plants have evolved an array for defense mechanisms, a general basal response followed by a specific adaptative response. In turn pathogens have evolved strategies to overcome the plant defense response. Most viruses encode viral suppressors of RNA silencing (VSRs) to counter plant antiviral response. P19 of tombusviruses, a well-studied VSR, functions by sequestering sRNAs, guides required for successful implementation of RNA silencing. HCPro, potyviral VRS, can act either directly by sequestering small RNAs or indirectly by interacting with host proteins to suppress anti-viral response (Revers and García, 2015). Viral-host protein interactions are specific – absence of a single host factor may confer resistance against one virus but not the other. For example, mutants of Suppressor of Gene Silencing 3 (SGS3), a cofactor involved in RNA silencing, display severe symptoms when challenged with *Cucumber Mosaic Virus* (CMV) but do not show any difference in their viral symptoms during TuMV or *Turnip Vein-Clearing Virus* (TVCV) infections (Csorba *et al.*, 2015). On the other hand, unavailability of a particular host factor can bring about an anti-viral response that is conserved across certain viral families. Mutants of AGO1 and AGO2, core components of RNA silencing pathway, were shown to be hypersusceptible to virus infections like CMV, TuMV or *Turnip Crinkle Virus* (TCV) (Csorba *et al.*, 2015). Therefore, anti-viral role of a particular response may or may not be conversed across different viral families.

In this chapter, we test if the role of s-nitrosylation is conserved by assessing *gsnor1-3* anti-viral response against CMV, a virus that does not belong to potyviral family. CMV belongs to genus *Cucumovirus* in the family *Bromoviridae.* CMV genome is encoded by three positive- stranded RNA. RNA1 and RNA2 code for viral RNA-dependent RNA polymerase subunits, 1a and 2a proteins, respectively. Subgenomic RNA4A derived from RNA2 encodes 2b protein, a VSR involved in viral virulence and systemic infection. Bicistronic RNA3 encodes Movement Protein (MP) and CP, required for viral cell-to-cell and systemic movement, respectively (Jacquemond, 2012). CMV is agriculturally significant species as it can infect more than 1000 species of plants which includes both monocots and dicots.

6.2. Results

6.2.1 CMV susceptibility test

4-week-old Col-0 and *gsnor1-3* plants were rub inoculated with CMV infectious sap to test the plant viral response against CMV. The inoculated plants were monitored for 3 weeks with periodic sample collection. As in case with TuMV susceptibility test (Section 3.2.2), 9 inoculated plants were randomly selected and pooled together to form one sample at each time point.

CMV infection followed the same infection pattern in both Col-0 and *gsnor1-3* plants. Though, viral infection symptoms were not obvious at 7 dpi, severe stunted growth was observed at 14 dpi, followed by recovery at 21 dpi. Visual observation of symptoms indicated that almost all plants were infected at 14 dpi in both genotypes (Figure 6.1A, B). Similarity in viral infection pattern was further confirmed by quantification of viral RNA in inoculated plants by qRT-PCR. Primers were designed for CMV RNA1 and CMV CP which is coded by CMV RNA3. Figure 6.1C, D indicate that the viral load in Col-0 and *gsnor1-3* is similar at all 3 time points with no significant difference (Student's *t*-test). The data suggests that *gsnor1-3* displays no resistance to CMV infection.

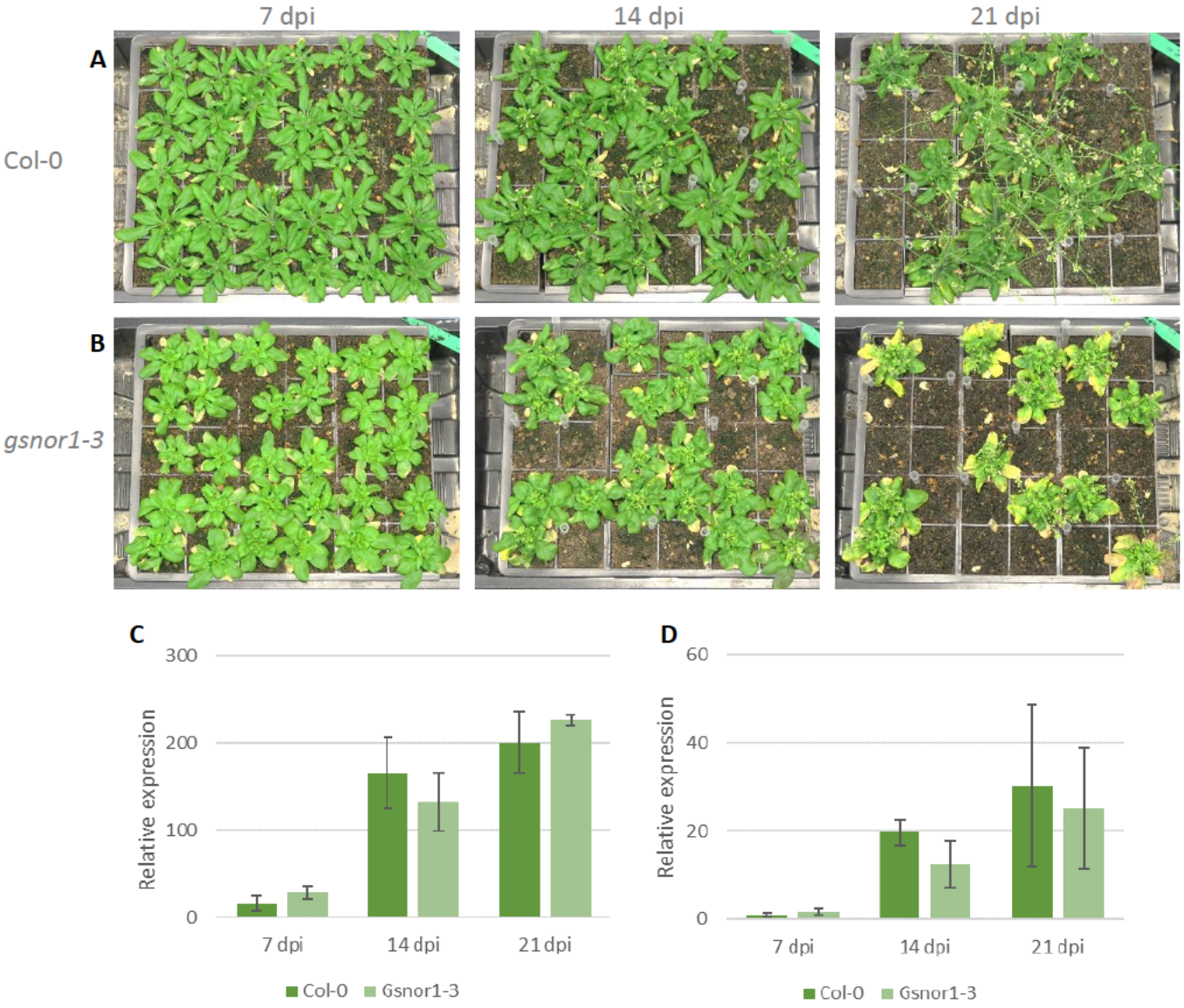

Figure 6.1 CMV susceptibility assay. Col-0 (A) and *gsnor1-3* (B) rub inoculated with CMV infectious sap were monitored for 3 weeks. Images were taken (A, B) and samples were collected at 7 dpi, 14 dpi and 21dpi. Randomly selected 9 plants were pooled together to form one sample. Viral RNA was quantified in these samples via qRT-PCR using primers for CMV RNA1 (C) and CMV CP (D). EF1a was used as reference gene. Error bars indicate SD of three replicates.

6.3 Discussion

CMV susceptibility assay demonstrated that the anti-viral response observed in *gsnor1-3* against TuMV, is not a conserved response against all viruses. Extent and pattern of CMV infection in *gsnor1-3* is very similar to Col-0 (Figure 6.1C, D) suggesting that the varied level of SNO in *gsnor1-3* does not influence CMV viral infection. It is not uncommon for different viral families to make use of different host proteins and have different mechanisms to escape plant immune response (discussed in section 6.1). However, if the observed viral resistance were purely based on *gsnor1-3* morphology then the response would have been broad spectrum. This highlights that the morphological features of *gsnor1-3* alone are not responsible for viral resistance. There is likely a SNO-based molecular mechanism involved that confers resistance against TuMV but not CMV.

The insensitivity of CMV to SA in the early stages of infection needs to be considered in the *gsnor1-3* viral response against CMV. Previous studies have shown that CMV is able to evade RNA silencing and SA mediated anti-viral response (Ji and Ding, 2001; Diaz-Pendon *et al.*, 2007; Zhou *et al.*, 2014). CMV replication and local infection was unaffected by SA-treatment (Naylor *et al.*, 1998; Singh *et al.*, 2004), while CMV-Δ2b (CMV mutant that does not express 2b) accumulation was reduced three-fold (Ji and Ding, 2001). This indicates role of CMV VSR 2b in evading SA mediated anti-viral response. However, SA is shown to effect CMV systemic movement resulting in delayed viral spread and symptom development (Naylor *et al.*, 1998). On the other hand, TuMV accumulation is inhibited by SA treatment (Peng *et*

al., 2013). The difference in response to CMV and TuMV observed here may be due to the extent of SA involvement in these two viruses.

Symptom recovery from CMV infection observed here is in line with previous studies carried out in *Arabidopsis* and *N.benthamiana*. CMV Fny strain, used in this study was shown to infect shoot apical meristems (SAM) transiently. It was then excluded from the shoot apices leading to symptom recovery (Zhang *et al.*, 2017). Symptom recovery was associated with reduced viral load at later stages of infection i.e., 35 - 56 dpi. This was due to reduced accumulation in CMV VSR 2b in SAM resulting in rescue of anti-viral RNA silencing (Zhang *et al.*, 2017). Symptom recovery is also observed during infections caused by other viruses such as *Cucurbit leaf crumple virus* (CuLCrV), *Tobacco Etch Virus* (TEV), *Tomato Black Ring Virus* (TBRV), *Tobacco Ringspot Virus* (TRSV) (Lindbo *et al.*, 1993; Ratcliff *et al.*, 1997; Hagen *et al.*, 2008; Siddiqui *et al.*, 2008). Expression of potyviral VSR HC-Pro, prevented symptom recovery in plants infected with TRSV, while expression of CMV 2b resulted only in partial recovery (Siddiqui *et al.*, 2008), suggesting that symptom recovery depends on the ability of the virus to counteract RNA silencing efficiently.

Chapter 7: Conclusions and future outlook

Plant pathogens are seen as important reducers of crop performances, impacting ecological, agronomical, and economic sustainability, all contributing to the problem of food security. Despite efforts to increase food production via improved pest and disease management, pathogens claim 10-16% of the global harvest (Chakraborty and Newton, 2011). Over the last few years, there has been a rise in the number of diseases caused by viral, bacterial, and fungal infections. Depending on the environmental conditions, these infections can reach 70–80% of the total plant population and cause up to 80–98% yield loss (Nazarov *et al.*, 2020). Viral infections make up 47% of the new emerging diseases affecting plants (Anderson *et al.*, 2004). As strict intracellular pathogens, viruses cannot be controlled chemically. Therefore, measures to prevent the spread of infection involve the destruction of infected plants and excessive pesticide applications to limit the population of vector organisms. Crop genetic resistances, which rely on knowledge of plant–virus interactions, are an effective alternative commonly used in agriculture (Nicaise, 2014).

This study aims to gain a deeper understanding of how plant-viral interactions are regulated. We focus on S-nitrosylation, a post-translational modification known to play an important role in plant immunity. A better understanding of plant-viral interactions can be used to develop methods to face viral attacks in fields and curb yield loss.

7.1 Increased SNO content leads to higher resistance against TuMV.

Over the past decade role of S-nitrosylation in plant immunity is becoming increasingly evident. SNO formation and turnover have been shown to regulate multiple modes of plant immunity. This is evident in plants with deviant SNO levels which display susceptibility to biotrophic pathogens (bacteria, fungus, and oomycete) (Feechan *et al.*, 2005; Rasul *et al.*, 2012). We discovered an opposing function of increased SNO in this research, namely resistance against a biotrophic pathogen. Plants with higher SNO levels (gsnor1-3, nox1) have a delayed onset of TuMV infection (Section 3.). This is consistent with a recent analysis of *N. tabacum* GSNOR knockout plants that showed viral resistance against TMV (Li *et al.*, 2021).

GSNO and NO have been shown to function through distinct pathways. Expression of denitrosylase, TRXh5 in *gsnor1-3* and *nox1* rescued the susceptibility phenotype in *nox1* but not in *gsnor1-3* (Kneeshaw *et al.*, 2014, Section 3.3). Furthermore, *gsnor1-3 nox1* double mutants allow for higher bacterial titers than either of the corresponding single mutants (Yun *et al.*, 2016b). Both studies show overlapping but distinct control by GSNO and NO signaling pathways. It is, therefore, possible that regulation of viral infection is different in *gsnor1-3* and *nox1.* Since we concentrate on *gsnor1-3* in this thesis, the conclusions drawn here are more applicable to the GSNO signaling pathway.

7.2 Delayed systemic movement contributes to increased TuMV resistance in *gsnor1-3*.

To understand the molecular mechanism associated with the delayed onset of TuMV infection, we looked at different stages of viral infection in *gsnor1-3* mutants. We hypothesized the delayed onset to be associated with the inhibition of initial stages of viral infection – replication and cell to cell movement. Measuring the rate of viral replication in protoplasts revealed that viral replication in *gsnor1-3* was not only uninhibited but encouraged, even though the plants had a lower viral load at an early time point (Figure 3.4B). A similar pattern was observed in the *PcaP1* mutant (Vijayapalani *et al.*, 2012) suggesting disruption of intracellular viral transport. If this was the case it was not reflected in local infection since the cell-to-cell movement in *gsnor1-3* was comparable to Col-0. Analysis of replication in Col-0 protoplasts in the presence of NO donors or inhibitors could aid in the discovery of more concrete answers. Additional research into cellular components involved in TuMV movement, such as the actin-myosin network, may be needed. In contrast with local movement, a significant delay in the viral spread at 7 dpi was observed on the evaluation of systemic movement of TuMV.

The study of host characteristics such as PD number, vascular pattern, and phloem transport rate provided insight into potential contributing factors to delayed systemic movement. A reduction in the number of complex PD had no effect on cell-to-cell movement in *gsnor1-3*. However, an underdeveloped vasculature and reduced phloem rate could in part explain slower TuMV systemic movement observed in *gsnor1-3*. Interestingly, CMV infection progression does not seem to be

hindered by these host features. This may imply that either these characteristics do not play a significant role in viral infection or that they are specific to TuMV. Taking a step further, it could imply that a TuMV compatible host factor(s) are affected by nitrosylation while CMV compatible host factors are not.

7.3 Future outlook

Through this project, we have established that S-nitrosylation influences TuMV infection progression. Further research is needed to identify the underlying molecular mechanism. Since viral infection is a multi-step process, we aimed to narrow down the possible targets by pinpointing the exact step of viral infection that is hindered in *gsnor1-3*. Sample collection with a focus on the establishment of TuMV infection in *gsnor1-3* and its systemic spread could help identify S-nitrosylation targets using proteomics approach.

The percentage of *gsnor1-3* plants infected by TuMV increased from 50% at 7 dpi to 80% at 21 dpi (Section 3.2.2), suggesting that the onset of the disease is delayed in some plants more than the others. Though the initial stages of infection are seemingly unaffected by the elevated level of SNO in *gsnor1-3*, the establishment of infection might be a different case. Analysis of inoculated leaves for S-nitrosylation candidates could shed light on viral infection establishment in *gsnor1-3*. Since S-nitrosylation is known to influence cell death (Yun *et al.*, 2011), PCD in *gsnor1-3* could be an interesting subject to explore regarding TuMV infections.

Plasmodesmata are essential host components involved in viral movement. No variation in the cell-to-cell movement was observed despite the reduced number of PD in *gsnor1-3* (Figure 4.5, 4.6). This highlights the need to further investigate PD structure and function in *gsnor1-3* plants. Structural analysis of PD under an electronic microscope can reveal any variation in *gsnor1-3* PD structure likely due to S-nitrosylation. Testing PD permeability in *gsnor1-3* by analysing callose deposition at PD or movement of free-GFP from a single cell (Kong *et al.*, 2012; Sager and Lee, 2018) can aid in understanding cell-to-cell movement in *gsnor1-3*.

S-nitrosylation of various viral proteins such as proteases, reverse transcriptase, ribonucleotide reductase, and nucleocapsid protein, have been shown to regulate viral infection in the mammalian system (Colasanti *et al.*, 1999). Computational analysis of TuMV proteins using GPS-SNO showed VSR HC-Pro to be a likely nitrosylation candidate. Experimental confirmation of the same could explain enhanced resistance as HC-Pro is involved in the suppression of host immune response.

7.4 Concluding remarks

This work serves as a starting point for further research into S-nitrosylation-based anti-viral responses. Future work carried on any of the multiple avenues listed here can lead to a better understanding of how redox signaling regulates viral infection. This, in turn, can lead to the identification of either genetic or ectopic

methods for disease control, bringing us one step closer to reducing yield loss due to viral infections.

References

Anderson, P. K., Cunningham, A. A., Patel, N. G., Morales, F. J., Epstein, P. R. and Daszak, P. (2004) Emerging infectious diseases of plants: Pathogen pollution, climate change and agrotechnology drivers.*Trends in Ecology and Evolution*, **19**(10), 535–544.

Astier, J., Gross, I. and Durner, J. (2018) Nitric oxide production in plants: An update.*Journal of Experimental Botany*, **69**(14), 3401–3411.

Baulcombe, D. (2004) RNA silencing in plants.*Nature*, **431**, 356–363.

Baumberger, N. and Baulcombe, D. C. (2005) Arabidopsis ARGONAUTE1 is an RNA Slicer that selectively recruits microRNAs and short interfering RNAs.*Proceedings of the National Academy of Sciences of the United States of America*, **102**(33), 11928–11933.

Begara-Morales, J. C., Chaki, M., Valderrama, R., Sánchez-Calvo, B., Mata-Pérez, C., Padilla, M. N., Corpas, F. J. and Barroso, J. B. (2018) Nitric oxide buffering and conditional nitric oxide release in stress response.*Journal of Experimental Botany*, **69**(14), 3425–3438.

Benhar, M., Forrester, M. T., Hess, D. T. and Stamler, J. S. (2008) Regulated protein denitrosylation by cytosolic and mitochondrial thioredoxins.*Science*, **320**(5879), 1050–1054.

Benhar, M., Forrester, M. T. and Stamler, J. S. (2009) Protein denitrosylation: Enzymatic mechanisms and cellular functions.*Nature Reviews Molecular Cell Biology*, **10**(10), 721–732.

Benitez-Alfonso, Y., Cilia, M., San Roman, A., Thomas, C., Maule, A., Hearn, S. and Jackson, D. (2009) Control of Arabidopsis meristem development by thioredoxin-dependent regulation of intercellular transport.*Proceedings of the National Academy of Sciences of the United States of America*, **106**(9), 3615–3620.

Bennett, C. W. (1940) The Relation of Viruses to Plant Tissues.*The botanical review*, **6**(9), 427–473.

Bernstein, E., Caudy, A. A., Hammond, S. M. and Hannon, G. J. (2001) Role for a bidentate ribonuclease in the initiation step of RNA interference.*Nature*, **409**, 363–366.

Bhardwaj, V., Meier, S., Petersen, L. N., Ingle, R. A. and Roden, L. C. (2011) Defence responses of arabidopsis thaliana to infection by pseudomonas syringae are

regulated by the circadian clock.*PLoS ONE*, **6**(10), 1–8.

Bühler, J., Rishmawi, L., Pflugfelder, D., Huber, G., Scharr, H., Hülskamp, M., Koornneef, M., Schurr, U. and Jahnke, S. (2015) Phenovein—a tool for leaf vein segmentation and analysis.*Plant Physiology*, **169**(4), 2359–2370.

Burch-Smith, T. M. and Zambryski, P. C. (2012) Plasmodesmata paradigm shift: Regulation from without versus within.*Annual Review of Plant Biology*, **63**, 239–260.

Cao, N., Zhan, B. and Zhou, X. (2019) Nitric oxide as a downstream signaling molecule in brassinosteroid-mediated virus susceptibility to maize chlorotic mottle virus in maize.*Viruses*, **11**(4), 368.

Carbonell, A., Fahlgren, N., Garcia-Ruiz, H., Gilbert, K. B., Montgomery, T. A., Nguyen, T., Cuperus, J. T. and Carrington, J. C. (2012) Functional analysis of three Arabidopsis argonautes using slicer-defective mutants.*The Plant Cell*, **24**(9), 3613–3629.

Cecconi, D., Orzetti, S., Vandelle, E., Rinalducci, S., Zolla, L. and Delledonne, M. (2009) Protein nitration during defense response in Arabidopsis thaliana.*Electrophoresis*, **30**(14), 2460–2468.

Chaki, M., Kovacs, I., Spannagl, M. and Lindermayr, C. (2014) Computational prediction of candidate proteins for S-nitrosylation in arabidopsis thaliana.*PLoS ONE*, **9**(10).

Chakraborty, S. and Newton, A. C. (2011) Climate change, plant diseases and food security: An overview.*Plant Pathology*, **60**(1), 2–14.

Chen, R. *et al.* (2009) The Arabidopsis paraquat resistant2 gene encodes an S-nitrosoglutathione reductase that is a key regulator of cell death.*Cell Research*, **19**(12), 1377–1387.

Cheng, X., Xiong, R., Li, Y., Li, F., Zhou, X. and Wang, A. (2017) Sumoylation of turnip mosaic virus RNA polymerase promotes viral infection by counteracting the host NPR1-mediated immune response.*Plant Cell*, **29**(3), 508–525.

Chisholm, S. T., Parra, M. A., Anderberg, R. J. and Carrington, J. C. (2001) Arabidopsis RTM1 and RTM2 genes function in phloem to restrict long-distance movement of tobacco etch virus.*Plant Physiology*, **127**(4), 1667–1675.

Chung, B. Y. W., Miller, W. A., Atkins, J. F. and Firth, A. E. (2008) An overlapping essential gene in the Potyviridae.*Proceedings of the National Academy of Sciences of the United States of America*, **105**(15), 5897–5902.

Colasanti, M., Persichini, T., Venturini, G. and Ascenzi, P. (1999) S-nitrosylation of viral proteins: Molecular bases for antiviral effect of nitric oxide.*IUBMB Life*, **48**(1), 25–31.

Covington, M. F., Maloof, J. N., Straume, M., Kay, S. A. and Harmer, S. L. (2008) Global transcriptome analysis reveals circadian regulation of key pathways in plant growth and development.*Genome Biology*, **9**(8).

Csorba, T., Kontra, L. and Burgyán, J. (2015) Viral silencing suppressors: Tools forged to fine-tune host-pathogen coexistence.*Virology*, **479**–**480**, 85–103.

Cui, X., Yaghmaiean, H., Wu, G., Wu, X., Chen, X., Thorn, G. and Wang, A. (2017) The C-terminal region of the Turnip mosaic virus P3 protein is essential for viral infection via targeting P3 to the viral replication complex.*Virology*, **510**(July), 147–155.

Dangl, J. L. and Jones, J. D. G. (2001) Defence Responses To Infection.*Nature*, **411**(June).

Das, K. and Roychoudhury, A. (2014) Reactive oxygen species (ROS) and response of antioxidants as ROS-scavengers during environmental stress in plants.*Frontiers in Environmental Science*, **2**(DEC), 1–13.

Delledonne, M., Xia, Y., Dixon, R. A. and Lamb, C. (1998) Nitric oxide functions asa signal in plant disease resistance.*Nature*, **394**, 585–588.

Delledonne, M., Zeier, J., Marocco, A. and Lamb, C. (2001) Signal interactions between nitric oxide and reactive oxygen intermediates in the plant hypersensitive disease resistance response.*Proceedings of the National Academy of Sciences of the United States of America*, **98**(23), 13454–13459.

Derrien, B., Baumberger, N., Schepetilnikov, M., Viotti, C., Cillia, J. De, Ziegler-graff, V., Isono, E., Schumacherb, K. and Genschik, P. (2012) Degradation of the antiviral component ARGONAUTE1 by the autophagy pathway.*PNAS*, **109**, 15942–15946.

Desikan, R., Griffiths, R., Hancock, J. and Neill, S. (2002) A new role for an old enzyme: Nitrate reductase-mediated nitric oxide generation is required for abscisic acid-induced stomatal closure in Arabidopsis thaliana.*Proceedings of the National Academy of Sciences of the United States of America*, **99**(25), 16314–16318.

Diaz-Pendon, J. A., Li, F., Li, W. X. and Ding, S. W. (2007) Suppression of antiviral silencing by cucumber mosaic virus 2b protein in Arabidopsis is associated with drastically reduced accumulation of three classes of viral small

interfering RNAs.*Plant Cell*, **19**(6), 2053–2063.

Domingos, P., Prado, A. M., Wong, A., Gehring, C. and Feijo, J. A. (2015) Nitric oxide: A multitasked signaling gas in plants.*Molecular Plant*, **8**(4), 506–520.

Dunoyer, P., Thomas, C., Harrison, S., Revers, F. and Maule, A. (2004) A Cysteine-Rich Plant Protein Potentiates Potyvirus Movement through an Interaction with the Virus Genome-Linked Protein VPg.*Journal of Virology*, **78**(5), 2301–2309.

Ehlers, K. and Kollmann, R. (2001) Primary and secondary plasmodesmata: Structure, origin, and functioning: Review article.*Protoplasma*, **216**(1–2), 1–30.

Fares, A., Rossignol, M. and Peltier, J. B. (2011) Proteomics investigation of endogenous S-nitrosylation in Arabidopsis.*Biochemical and Biophysical Research Communications,* **416** ,331–336.

Feechan, A., Kwon, E., Yun, B.-W., Wang, Y., Pallas, J. A. and Loake, G. J. (2005) A central role for S-nitrosothiols in plant disease resistance.*Proceedings of the National Academy of Sciences*, **102**, 8054–8059.

Feng, J., Chen, L. and Zuo, J. (2019) Protein S-Nitrosylation in plants: Current progresses and challenges.*Journal of Integrative Plant Biology*, **61**(12), 1206–1223.

Ferreira, L. C. and Cataneo, A. C. (2010) Nitric oxide in plants: a brief discussion on this multifunctional molecule.*Scientia Agricola*, **67**(2), 236–243.

Fitzgibbon, J., Beck, M., Zhou, J., Faulkner, C., Robatzek, S. and Oparka, K. (2013) A developmental framework for complex plasmodesmata formation revealed by large-scale imaging of the arabidopsis leaf epidermis.*Plant Cell*, **25**(1), 57–70.

Frungillo, L., Skelly, M. J., Loake, G. J., Spoel, S. H. and Salgado, I. (2014) S-nitrosothiols regulate nitric oxide production and storage in plants through the nitrogen assimilation pathway.*Nature Communications*, **5**, 5401.

Fu, Z. Q. and Dong, X. (2013) Systemic Acquired Resistance: Turning Local Infection into Global Defense.*Annual Review of Plant Biology*, **64**(1), 839–863.

Garcia-Ruiz, H., Takeda, A., Chapman, E. J., Sullivan, C. M., Fahlgren, N., Brempelis, K. J. and Carrington, J. C. (2010) Arabidopsis RNA-dependent RNA polymerases and dicer-like proteins in antiviral defense and small interfering RNA biogenesis during Turnip mosaic virus infection.*Plant Cell*, **22**(2), 481–496.

Garcia-Ruiz, H. (2018) Susceptibility genes to plant viruses.*Viruses*, **10**(9).

Gergerich, R. C. and Dolja, V. V. (2006) Introduction to Plant Viruses, the Invisible Foe.*The Plant Health Instructor*.

Grant, J. J. and Loake, G. J. (2000) Role of Reactive Oxygen Intermediates and Cognate Redox Signaling in Disease Resistance.*Plant Physiology*, **124**, 21–29.

Guerra, D., Ballard, K., Truebridge, I. and Vierling, E. (2016) S-nitrosation of conserved cysteines modulates activity and stability of S-nitrosoglutathione reductase (GSNOR).*Biochemistry*, **55**(17), 2452–2464.

Hagen, C., Rojas, M. R., Kon, T. and Gilbertson, R. L. (2008) Recovery from Cucurbit leaf crumple virus (Family Geminiviridae, Genus Begomovirus) infection is an adaptive antiviral response associated with changes in viral small RNAs.*Phytopathology*, **98**(9), 1029–1037.

Han, G. Z. (2019) Origin and evolution of the plant immune system.*New Phytologist*, **222**(1), 70–83.

He, Y. *et al.* (2004) Nitric Oxide Represses the Arabidopsis Floral Transition.*Science*, **305**, 1968–1971.

Hipper, C., Brault, V., Ziegler-Graff, V. and Revers, F. (2013) Viral and cellular factors involved in phloem transport of plant viruses.*Frontiers in Plant Science*, **4**(MAY), 1–24.

Holmgren, A. and Bjornstedt, M. (1995) Thioredoxin and thioredoxin reductase.*Methods in Enzymology*, **252**, 199–208.

Hou, S., Liu, Z., Shen, H. and Wu, D. (2019) Damage-associated molecular pattern-triggered immunity in plants.*Frontiers in Plant Science*, **10** , 646.

Hu, J., Huang, X., Chen, L., Sun, X., Lu, C., Zhang, L., Wang, Y. and Zuo, J. (2015) Site-specific nitrosoproteomic identification of endogenously S-nitrosylated proteins in Arabidopsis.*Plant Physiology*, **167**(4), 1731–1746.

Hua, J. (2013) Modulation of plant immunity by light, circadian rhythm, and temperature.*Current Opinion in Plant Biology*, **16**(4), 406–413.

Huang, D., Huo, J., Zhang, J., Wang, C., Wang, B., Fang, H. and Liao, W. (2019) Protein S-nitrosylation in programmed cell death in plants.*Cellular and Molecular Life Sciences*, **76**(10), 1877–1887.

Huber, S. C. and Hardin, S. C. (2004) Numerous posttranslational modifications provide opportunities for the intricate regulation of metabolic enzymes at multiple levels.*Current Opinion in Plant Biology*, 7:318-322.

Hunold, R., Bronner, R. and Hahne, G. (1994) Early events in microprojectile bombardment: cell viability and particle location.*The Plant Journal*, **5**(4), 593–604.

Ishii, S. (1987) Generation of active oxygen species during enzymic isolation of protoplasts from oat leaves.*In Vitro Cellular & Developmental Biology*, **23**(9), 653–658.

Ivanov, K. I., Puustinen, P., Merits, A., Saarma, M. and Mäkinen, K. (2001) Phosphorylation Down-regulates the RNA Binding Function of the Coat Protein of Potato Virus A.*Journal of Biological Chemistry*, **276**(17), 13530–13540.

Ivanov, K. I., Puustinen, P., Gabrenaite, R., Vihinen, H., Rönnstrand, L., Valmu, L., Kalkkinen, N. and Mäkinen, K. (2003) Phosphorylation of the potyvirus capsid protein by protein kinase CK2 and its relevance for virus infection.*Plant Cell*, **15**(9), 2124–2139.

Ivanov, K. I., Eskelin, K., Lõhmus, A. and Mäkinen, K. (2014) Molecular and cellular mechanisms underlying potyvirus infection.*Journal of General Virology*, **95**(PART 7), 1415–1429.

Jacquemond, M. (2012) *Cucumber Mosaic Virus*. 1st edn.*Advances in Virus Research*. 1st edn. Elsevier Inc.

Ji, L. H. and Ding, S. W. (2001) The suppressor of transgene RNA silencing encoded by Cucumber mosaic virus interferes with salicylic acid-mediated virus resistance.*Molecular Plant-Microbe Interactions*, **14**(6), 715–724.

Kanyuka, K. and Rudd, J. J. (2019) Cell surface immune receptors: the guardians of the plant's extracellular spaces.*Current Opinion in Plant Biology*, **50**, 1–8.

Karapetyan, S. and Dong, X. (2018) Redox and the circadian clock in plant immunity: A balancing act.*Free Radical Biology and Medicine*, **119**(December 2017), 56–61.

Kawabe, H., Ohtani, M., Kurata, T., Sakamoto, T. and Demura, T. (2018) Protein S-Nitrosylation Regulates Xylem Vessel Cell Differentiation in Arabidopsis.*Plant & cell physiology*, **59**(1), 17–29.

Kebrom, T. H. (2017) A growing stem inhibits bud outgrowth – The overlooked theory of apical dominance.*Frontiers in Plant Science*, **8**(October), 1–7.

Kneeshaw, S., Gelineau, S., Tada, Y., Loake, G. J. and Spoel, S. H. (2014) Selective protein denitrosylation activity of thioredoxin-h5 modulates plant

immunity.*Molecular Cell*, **56**(1), 153–162.

Knox, K., Paterlini, A., Thomson, S. and Oparka, K. (2018) The coumarin glucoside, esculin, reveals rapid changes in phloem-transport velocity in response to environmental cues1.*Plant Physiology*, **178**(2), 795–807.

Kolbert, Z., Feigl, G., Bordé, Á., Molnár, Á. and Erdei, L. (2017) Protein tyrosine nitration in plants: Present knowledge, computational prediction and future perspectives.*Plant Physiology and Biochemistry*, **113**(2), 56–63.

Kolbert, Z. and Erdei, L. (2008) Involvement of nitrate reductase in auxin-induced NO synthesis.*Plant Signaling and Behavior*, **3**(11), 972–973.

Kong, D., Karve, R., Willet, A., Chen, M. K., Oden, J. and Shpak, E. D. (2012) Regulation of plasmodesmatal permeability and stomatal patterning by the glycosyltransferase-like protein kobito1.*Plant Physiology*, **159**(1), 156–168.

Kortemme, T., Darby, N. J. and Creighton, T. E. (1996) Electrostatic interactions in the active site of the N-terminal thioredoxin-like domain of protein disulfide isomerase.*Biochemistry*, **35**(46), 14503–14511.

Kovacs, I. and Lindermayr, C. (2013) Nitric oxide-based protein modification: Formation and site-specificity of protein S-nitrosylation.*Frontiers in Plant Science*, **4**(MAY), 1–10.

Kwon, E., Feechan, A., Yun, B. W., Hwang, B. H., Pallas, J. A., Kang, J. G. and Loake, G. J. (2012) AtGSNOR1 function is required for multiple developmental programs in Arabidopsis.*Planta*, **236**(3), 887–900.

Lai, A. G., Doherty, C. J., Mueller-Roeber, B., Kay, S. A., Schippers, J. H. M. and Dijkwel, P. P. (2012) Circadian Clock-Associated 1 regulates ROS homeostasis and oxidative stress responses.*Proceedings of the National Academy of Sciences of the United States of America*, **109**(42), 17129–17134.

Lamb, C. and Dixon, R. A. (1997) The oxidative burst in plant disease r esistance.*Annual Review of Plant Biology*, **48**, 251–275.

Lee, H. A. *et al.* (2017) Current understandings of plant nonhost resistance.*Molecular Plant-Microbe Interactions*, **30**(1), 5–15.

Lee, J. Y. *et al.* (2011) A plasmodesmata-localized protein mediates crosstalk between cell-to-cell communication and innate immunity in arabidopsis.*Plant Cell*, **23**(9), 3353–3373.

Lellis, A. D., Kasschau, K. D., Whitham, S. A. and Carrington, J. C. (2002) Loss-of-susceptibility mutants of Arabidopsis thaliana reveal an essential role for

eIF(iso)4E during potyvirus infection.*Current Biology*, **12**(12), 1046–1051.

Léonard, S., Plante, D., Wittmann, S., Daigneault, N., Fortin, M. G. and Laliberté, J.-F. (2000) Complex Formation between Potyvirus VPg and Translation Eukaryotic Initiation Factor 4E Correlates with Virus Infectivity.*Journal of Virology*, **74**(17), 7730– 7737.

Li-Juan, Z. *et al.* (2018) Nitric oxide as a signaling molecule in brassinosteroid-mediated virus resistance to Cucumber mosaic virus in Arabidopsis thaliana.*Physiologia Plantarum*, **163**, 196–210.

Li, G., Lv, H., Zhang, S., Zhang, S., Li, F., Zhang, H., Qian, W., Fang, Z. and Sun, R. (2019) TuMV management for brassica crops through host resistance: retrospect and prospects.*Plant Pathology*, **68**(6), 1035–1044.

Li, Z. C., Ren, Q. W., Guo, Y., Ran, J., Ren, X. T., Wu, N. N., Xu, H. Y., Liu, X. and Liu, J. Z. (2021) Dual Roles of GSNOR1 in Cell Death and Immunity in Tetraploid Nicotiana tabacum.*Frontiers in Plant Science*, **12**(February), 1–13.

Lindbo, J. A., Silva-Rosales, L., Proebsting, W. M. and Dougherty, W. G. (1993) Induction of a highly specific antiviral state in transgenic plants: Implications for regulation of gene expression and virus resistance.*Plant Cell*, **5**(12), 1749–1759.

Lindermayr, C., Sell, S., Müller, B., Leister, D. and Durner, J. (2010) Redox regulation of the NPR1-TGA1 system of Arabidopsis thaliana by nitric oxide.*Plant Cell*, **22**(8), 2894–2907.

Lindermayr, C., Saalbach, G. and Durner, J. (2005) Proteomic Identification of S -Nitrosylated Proteins in Arabidopsis.*Plant Physiology*, **137**(March 2005), 921–930.

Liu, J.-Z. *et al.* (2015) Loss of GSNOR1 Function Leads to Compromised Auxin Signaling and Polar Auxin Transport.*Molecular Plant*, **8**(9), 1350–1365.

Liu, Y., Ren, D., Pike, S., Pallardy, S., Gassmann, W. and Zhang, S. (2007) Chloroplast-generated reactive oxygen species are involved in hypersensitive response-like cell death mediated by a mitogen-activated protein kinase cascade.*Plant Journal*, **51**(6), 941–954.

Mäkinen, K. and Hafrén, A. (2014) Intracellular coordination of potyviral RNA functions in infection.*Frontiers in Plant Science*, **5**(MAR), 1–12.

Mannick, J. B., Asano, K., Izumi, K., Kieff, E. and Stamler, J. S. (1994) Nitric oxide produced by human B lymphocytes inhibits apoptosis and Epstein-Barr virus

reactivation.*Cell*, **79**(7), 1137–1146.

Mata-Pérez, C. and Spoel, S. H. (2019) Thioredoxin-mediated redox signalling in plant immunity.*Plant Science*, **279**(May 2018), 27–33.

Meyer, Y., Siala, W., Bashandy, T., Riondet, C., Vignols, F. and Reichheld, J. P. (2008) Glutaredoxins and thioredoxins in plants.*Biochimica et Biophysica Acta - Molecular Cell Research*, **1783**(4), 589–600.

Mittler, R., Vanderauwera, S., Gollery, M. and Van Breusegem, F. (2004) Reactive oxygen gene network of plants.*Trends in Plant Science*, **9**(10), 490–498.

Moreau, M., Gyu, I. L., Wang, Y., Crane, B. R. and Klessig, D. F. (2008) AtNOS/AtNOA1 is a functional Arabidopsis thaliana cGTPase and not a nitric-oxide synthase.*Journal of Biological Chemistry*, **283**(47), 32957–32967.

Mou, Z., Fan, W. and Dong, X. (2003) Inducers of plant systemic acquired resistance Regulate NPR1 function through redox changes.*Cell*, **113**(7), 935–944.

Mur, L. A. J., Kenton, P., Lloyd, A. J., Ougham, H. and Prats, E. (2008) The hypersensitive response; The centenary is upon us but how much do we know?*Journal of Experimental Botany*, **59**(3), 501–520.

Naylor, M., Murphy, A. M., Berry, J. O. and Carr, J. P. (1998) Salicylic acid can induce resistance to plant virus movement.*Molecular Plant-Microbe Interactions*, **11**(9), 860–868.

Nazarov, P. A., Baleev, D. N., Ivanova, M. I., Sokolova, L. M. and Karakozova, M. V. (2020) Infectious Plant Diseases: Etiology, Current Status, Problems and Prospects in Plant Protection.*Acta Naturae*, **12**(3), 46–59.

Newman, M. A., Sundelin, T., Nielsen, J. T. and Erbs, G. (2013) MAMP (microbe-associated molecular pattern) triggered immunity in plants.*Frontiers in Plant Science*, **4**(MAY), 1–14.

Nicaise, V. (2014) Crop immunity against viruses: Outcomes and future challenges.*Frontiers in Plant Science*, **5**(NOV), 1–18.

Nigam, D., LaTourrette, K., Souza, P. F. N. and Garcia-Ruiz, H. (2019) Genome-Wide Variation in Potyviruses.*Frontiers in Plant Science*, **10**(November), 1–28.

Ormenese, S., Havelange, A., Deltour, R. and Bernier, G. (2000) The frequency of plasmodesmata increases early in the whole shoot apical meristem of Sinapis alba L. during floral transition.*Planta*, **211**(3), 370–375.

Ormenese, S., Bernier, G. and Périlleux, C. (2006) Cytokinin application to the shoot

apical meristem of Sinapis alba enhances secondary plasmodesmata formation.*Planta*, **224**(6), 1481–1484.

Palevitz, B. A. and Hepler, P. K. (1985) Changes in dye coupling of stomatal cells of Allium and Commelina demonstrated by microinjection of Lucifer yellow.*Planta*, **164**(4), 473–479.

Peng, H., Li, S., Wang, L., Li, Ying, Li, Yanxiao, Zhang, C. and Hou, X. (2013) Turnip mosaic virus induces expression of the LRR II subfamily genes and regulates the salicylic acid signaling pathway in non-heading Chinese cabbage.*Physiological and Molecular Plant Pathology*, **82**, 64–72.

Pieterse, C. M. J., Leon-Reyes, A., Van Der Ent, S. and Van Wees, S. C. M. (2009) Networking by small-molecule hormones in plant immunity.*Nature Chemical Biology*, **5**(5), 308–316.

Pieterse, C. M. J., Van der Does, D., Zamioudis, C., Leon-Reyes, A. and Van Wees, S. C. M. (2012) Hormonal Modulation of Plant Immunity.*Annual Review of Cell and Developmental Biology*, **28**(1), 489–521.

Pyott, D. E., Sheehan, E. and Molnar, A. (2016) Engineering of CRISPR/Cas9-mediated potyvirus resistance in transgene-free Arabidopsis plants.*Molecular plant pathology*, **17**(8), 1276–1288.

Qi, J., Wang, J., Gong, Z. and Zhou, J. M. (2017) Apoplastic ROS signaling in plant immunity.*Current Opinion in Plant Biology*, **38**, 92–100.

Radford, J. E., Vesk, M. and Overall, R. L. (1998) Callose deposition at plasmodesmata.*Protoplasma*, **201**(1–2), 30–37.

Radford, J. E. and White, R. G. (1998) Localization of a myosin-like protein to plasmodesmata.*Plant Journal*, **14**(6), 743–750.

Rasul, S., Dubreuil-Maurizi, C., Lamotte, O., Koen, E., Poinssot, B., Alcaraz, G., Wendehenne, D. and Jeandroz, S. (2012) Nitric oxide production mediates oligogalacturonide-triggered immunity and resistance to Botrytis cinerea in Arabidopsis thaliana.*Plant, Cell and Environment*, **35**, 1483–1499.

Ratcliff, F., Harrison, B. D. and Baulcombe, D. C. (1997) A similarity between viral defense and gene silencing in plants.*Science*, **276**(5318), 1558–1560.

Revers, F. and García, J. A. (2015) *Molecular biology of potyviruses*. 1st edn.*Advances in Virus Research*. 1st edn. Elsevier Inc.

Riechmann, J. L., Lain, S. and Garcia, J. A. (1992) Highlights and prospects of potyvirus molecular biology.*Journal of General Virology*, **73**(1), 1–16.

Robards, A. W. and Lucas, W. J. (1990) Plasmodesmata.*Annu. Rev. Plant Physiol. Plant Mol. Biol.*, **41**, 36.

Roberts, A. G. and Oparka, K. J. (2003) Plasmodesmata and the control of symplastic transport.*Plant, Cell and Environment*, **26**(1), 103–124.

Rockel, P., Strube, F., Rockel, A., Wildt, J. and Kaiser, W. M. (2002) Regulation of nitric oxide (NO) production by plant nitrate reductase in vivo and in vitro.*Journal of Experimental Botany*, **53**(366), 103–110.

Romero-Puertas, M. C., Campostrini, N., Mattè, A., Righetti, P. G., Perazzolli, M., Zolla, L., Roepstorff, P. and Delledonne, M. (2008) Proteomic analysis of S-nitrosylated proteins in Arabidopsis thaliana undergoing hypersensitive response.*Proteomics*, **8**(7), 1459–1469.

Sager, R. E. and Lee, J.-Y. (2018) Plasmodesmata at a glance.*Journal of Cell Science*, **131**(11), jcs209346.

Sager, R. and Lee, J. Y. (2014) Plasmodesmata in integrated cell signalling: Insights from development and environmental signals and stresses.*Journal of Experimental Botany*, **65**(22), 6337–6358.

Sastry, S. K. and Zitter, T. A. (2014) *Plant Virus and Viroid Diseases in the Tropics. Vol 2. Epidemiology and management*.

Saura, M., Zaragoza, C., McMillan, A., Quick, R. A., Hohenadl, C., Lowenstein, J. M. and Lowenstein, C. J. (1999) An antiviral mechanism of nitric oxide: Inhibition of a viral protease.*Immunity*, **10**(1), 21–28.

Schulz, A. (1994) Phloem transport and differential unloading in pea seedlings after source and sink manipulations.*Planta*, **192**(2), 239–248.

Seligman, K., Saviani, E. E., Oliveira, H. C., Pinto-Maglio, C. A. F. and Salgado, I. (2008) Floral transition and nitric oxide emission during flower development in Arabidopsis thaliana is affected in nitrate reductase-deficient plants.*Plant and Cell Physiology*, **49**(7), 1112–1121.

Seta, A. *et al.* (2017) Post-translational regulation of the dicing activities of arabidopsis DICER-LIKE 3 and 4 by inorganic phosphate and the redox state.*Plant and Cell Physiology*, **58**(3), 485–495.

Shapiguzov, A., Vainonen, J. P., Wrzaczek, M. and Kangasjärvi, J. (2012) ROS-talk - how the apoplast, the chloroplast, and the nucleus get the message through.*Frontiers in Plant Science*, **3**(DEC), 1–9.

Shi, H., Ye, T., Zhu, J. K. and Chan, Z. (2014) Constitutive production of nitric oxide

leads to enhanced drought stress resistance and extensive transcriptional reprogramming in Arabidopsis.*Journal of Experimental Botany*, **65**(15), 4119–4131.

Siddiqui, S. A., Sarmiento, C., Kiisma, M., Koivumäki, S., Lemmetty, A., Truve, E. and Lehto, K. (2008) Effects of viral silencing suppressors on tobacco ringspot virus infection in two Nicotiana species.*Journal of General Virology*, **89**(6), 1502–1508.

Singh, D. P., Moore, C. A., Gilliland, A. and Carr, J. P. (2004) Activation of multiple antiviral defence mechanisms by salicylic acid.*Molecular Plant Pathology*, **5**, 57–63.

Singh, S. P., Wishnok, J. S., Keshive, M., Deen, W. M. and Tannenbaum, S. R. (1996) The chemistry of the S -nitrosoglutathione/ glutathione system.*Proc. Natl. Acad. Sci. U.S.A.*, **93**(December), 14428–14433.

Song, F. and Goodman, R. M. (2001) Activity of nitric oxide is dependent on, but is partially required for function of, salicylic acid in the signaling pathway in tobacco systemic acquired resistance.*Molecular Plant-Microbe Interactions*, **14**(12), 1458–1462.

Stonebloom, S., Burch-Smith, T., Kim, I., Meinke, D., Mindrinos, M. and Zambryski, P. (2009) Loss of the plant DEAD-box protein ISE1 leads to defective mitochondria and increased cell-to-cell transport via plasmodesmata.*Proceedings of the National Academy of Sciences of the United States of America*, **106**(40), 17229–17234.

Stonebloom, S., Brunkard, J. O., Cheung, A. C., Jiang, K., Feldman, L. and Zambryski, P. (2012) Redox states of plastids and mitochondria differentially regulate intercellular transport via plasmodesmata.*Plant Physiology*, **158**(1), 190–199.

Tada, Y., Spoel, S. H., Pajerowska-Mukhtar, K., Mou, Z., Song, J., Wang, C., Zuo, J. and Dong, X. (2008) Plant immunity requires conformational charges of NPR1 via S-nitrosylation and thioredoxins.*Science*, **321**, 5891.

Takahashi, M., Shigeto, J., Izumi, S., Yoshizato, K. and Morikawa, H. (2016) Nitration is exclusive to defense-related PR-1, PR-3 and PR-5 proteins in tobacco leaves.*Plant Signaling and Behavior*, **11**(7), 1–5.

Torres, M. A., Dangl, J. L. and Jones, J. D. G. (2002) Arabidopsis gp91phox homologues Atrbohd and Atrbohf are required for accumulation of reactive oxygen intermediates in the plant defense response.*Proceedings of the National Academy of Sciences of the United States of America*, **99**(1), 517–522.

Torres, M. A., Jones, J. D. G. and Dangl, J. L. (2006) Reactive oxygen species signaling in response to pathogens.*Plant Physiology*, **141**(2), 373–378.

Tripathy, B. C. and Oelmüller, R. (2012) Reactive oxygen species generation and signaling in plants.*Plant Signaling and Behavior*, **7**(12), 1621–1633.

Tun, N. N., Santa-Catarina, C., Begum, T., Silveira, V., Handro, W., Segal Floh, E. I. and Scherer, G. F. E. (2006) Polyamines induce rapid biosynthesis of nitric oxide (NO) in Arabidopsis thaliana seedlings.*Plant and Cell Physiology*, **47**(3), 346–354.

Urcuqui-Inchima, S., Haenni, A. L. and Bernardi, F. (2001) Potyvirus proteins: A wealth of functions.*Virus Research*, **74**(1–2), 157–175.

Vijayapalani, P., Maeshima, M., Nagasaki-Takekuchi, N. and Miller, W. A. (2012) Interaction of the trans-frame potyvirus protein P3N-PIPO with host protein PCaP1 facilitates potyvirus movement.*PLoS Pathogens*, **8**(4).

Voinnet, O., Vain, P., Angell, S. and Baulcombe, D. C. (1998) Systemic spread of sequence-specific transgene RNA degradation in plants is initiated by localized introduction of ectopic promoterless DNA.*Cell*, **95**(2), 177–187.

Voinnet, O. and Baulcombe, D. (1997) Systemic signalling in gene silencing.*Nature*, **389**, 553.

Walsh, J. A. and Jenner, C. E. (2002) Turnip mosaic virus and the quest for durable resistance.*Molecular Plant Pathology*, **3**, 289–300.

Wan, J., Cabanillas, D. G., Zheng, H. and Laliberté, J. F. (2015) Turnip mosaic virus moves systemically through both phloem and xylem as membrane-associated complexes.*Plant Physiology*, **167**(4), 1374–1388.

Wang, A. and Zhou, X. (2016) Current research topics in plant virology.*Current Research Topics in Plant Virology*, 153–172.

Wang, W., Barnaby, J. Y., Tada, Y., Li, H., Tör, M., Caldelari, D., Lee, D. U., Fu, X. D. and Dong, X. (2011) Timing of plant immune responses by a central circadian regulator.*Nature*, **470**(7332), 110–115.

Wang, Y., Yun, B. W., Kwon, E. J., Hong, J. K., Yoon, J. and Loake, G. J. (2006) S-nitrosylation: An emerging redox-based post-translational modification in plants.*Journal of Experimental Botany*, 57:1777-1784.

Wang, Y. Q. *et al.* (2009) S-nitrosylation of AtSABP3 antagonizes the expression of plant immunity.*Journal of Biological Chemistry*, **284**(4), 2131–2137.

Webb, A. A. R. (2003) The physiology of circadian rhythms in plants.*New Phytologist*, **160**(2), 281–303.

Wei, T., Zhang, C., Hong, J., Xiong, R., Kasschau, K. D., Zhou, X., Carrington, J. C. and Wang, A. (2010) Formation of complexes at plasmodesmata for potyvirus intercellular movement is mediated by the viral protein P3N-PIPO.*PLoS Pathogens*, **6**(6).

Wei, T. and Wang, A. (2008) Biogenesis of Cytoplasmic Membranous Vesicles for Plant Potyvirus Replication Occurs at Endoplasmic Reticulum Exit Sites in a COPI- and COPII-Dependent Manner.*Journal of Virology*, **82**(24), 12252–12264.

White, R. G., Badelt, K., Overall, R. L. and Vesk, M. (1994) Actin associated with plasmodesmata.*Protoplasma*, **180**(3–4), 169–184.

Wink, D. A., Hanbauer, I., Krishna, M. C., DeGraff, W., Gamson, J. and Mitchell, J. B. (1993) Nitric oxide protects against cellular damage and cytotoxicity from reactive oxygen species.*Proceedings of the National Academy of Sciences of the United States of America*, **90**(21), 9813–9817.

Wu, F. H., Shen, S. C., Lee, L. Y., Lee, S. H., Chan, M. T. and Lin, C. S. (2009) Tape-arabidopsis sandwich - A simpler arabidopsis protoplast isolation method.*Plant Methods*, **5**(1), 1–10.

Xiao, L., Zhang, L., Yang, G., Zhu, H. and He, Y. (2012) Transcriptome of protoplasts reprogrammed into stem cells in Physcomitrella patens.*PLoS ONE*, **7**(4).

Yu, M., Yun, B. W., Spoel, S. H. and Loake, G. J. (2012) A sleigh ride through the SNO: Regulation of plant immune function by protein S-nitrosylation.*Current Opinion in Plant Biology*, 424–430.

Yu, X., Feng, B., He, P. and Shan, L. (2017) From Chaos to Harmony: Responses and Signaling upon Microbial Pattern Recognition.*Annual Review of Phytopathology*, **55**(1), 109–137.

Yun, B. W., Feechan, A., Yin, M., Saidi, N. B., Le Bihan, T., Yu, M., *et al.* (2011) S-nitrosylation of NADPH oxidase regulates cell death in plant immunity.*Nature*, **478**(7368), 264–268.

Yun, B. W., Skelly, M. J., Yin, M., Yu, M., Mun, B. G., Lee, S. U., Hussain, A., Spoel, S. H. and Loake, G. J. (2016) Nitric oxide and S-nitrosoglutathione function additively during plant immunity.*The New phytologist*.

Zeng, L., Zhou, J., Li, B. and Xing, D. (2015) A high-sensitivity optical device for the

early monitoring of plant pathogen attack via the in vivo detection of ROS bursts.*Frontiers in Plant Science*, **6**(FEB), 1–8.

Zhang, X. P., Liu, D. S., Yan, T., Fang, X. D., Dong, K., Xu, J., Wang, Y., Yu, J. L. and Wang, X. B. (2017) Cucumber mosaic virus coat protein modulates the accumulation of 2b protein and antiviral silencing that causes symptom recovery in planta.*PLoS Pathogens*, **13**(7), 1–25.

Zhou, T., Murphy, A. M., Lewsey, M. G., Westwood, J. H., Zhang, H. M., González, I., Canto, T. and Carr, J. P. (2014) Domains of the cucumber mosaic virus 2b silencing suppressor protein affecting inhibition of salicylic acid-induced resistance and priming of salicylic acid accumulation during infection.*Journal of General Virology*, **95**(PART 6), 1408–1413.